

Evaluation of the Vertical Accuracy of Open Access Digital Elevation Models across Different Physiographic Regions and River Basins of Nepal

Saroj Karki¹, Suchana Acharya², and Ashok Gautam³

¹Ministry of Physical Infrastructure Development, Province-1, Nepal

²Department of Water Resources and Irrigation (DoWRI), Government of Nepal

³Ministry of Physical Infrastructure Development, Karnali Province, Province Government, Nepal

November 26, 2022

Abstract

The vertical accuracy of eight different freely accessible DEMs has been evaluated across different physiographic divisions and the river basins of Nepal. Results revealed that MERIT is superior to other DEMs (RMSE 9m) in the low-lying Terai plains of Nepal where the elevation range is lower. In High mountains and High Himalayas having higher elevation range, SRTM90m outperformed all its counterparts. Meanwhile, in Siwalik and middle mountains, both SRTM90m and HYDROSHEDS exhibited almost similar RMSE indicating their compatible uses in these regions. Meanwhile, the accuracy assessment across different river basins of Nepal discerned that the accuracy of SRTM90m was above others in larger river basins like Koshi (RMSE 224m), Narayani (RMSE 215m), and Karnali (RMSE 265m) where the range of elevation is greater. In the smaller to medium-sized basins like Kankai, Kamala, Bagmati, West Rapti, and Babai, HYDROSHEDS was preferable along with SRTM90m. Based on different error statistics, the DEMs were ranked in order of their accuracy.

Evaluation of the Vertical Accuracy of Open Access Digital Elevation Models across Different Physiographic Regions and River Basins of Nepal

Saroj Karki^{1*}, Suchana Acharya² and Ashok Gautam³

¹Ministry of Physical Infrastructure Development, Province-1, Province Government, Nepal

²Department of Water Resources and Irrigation (DoWRI), Government of Nepal

³Ministry of Physical Infrastructure Development, Karnali Province, Province Government, Nepal

(sarojioe@gmail.com)

ABSTRACT

The vertical accuracy of eight different freely accessible DEMs have been evaluated across different physiographic divisions and the river basins of Nepal. Results revealed that MERIT is superior to other DEMs (RMSE 9m) in the low lying Terai plains of Nepal where the elevation range is lower. In High mountains and High Himalayas having higher elevation range, SRTM90m outperformed all its counterpart. Meanwhile in Siwalik and middle mountains, both SRTM90m and HYDROSHEDS exhibited almost similar RMSE indicating their compatible uses in these regions. Meanwhile, the accuracy assessment across different river basins of Nepal discerned that the accuracy of SRTM90m was above others in larger river basins like Koshi (RMSE 224m), Narayani (RMSE 215m) and Karnali (RMSE 265m) where the range of elevation is greater. In the smaller to medium-sized basins like Kankai, Kamala, Bagmati, West Rapti and Babai, HYDROSHEDS was preferrable along with SRTM90m. Based on different error statistics, the DEMs were ranked in order of their accuracy.

Keywords: Digital Elevation Models, Terai, Chure, Nepal, River basins.

1. INTRODUCTION

Digital Elevation Models (DEMs) that represent the surface elevation are fundamental to any studies that deal with the earth and environmental science (Jing et al. 2014). DEMs are established as a principal spatial dataset for different hydro-environmental and geosciences applications (Schumann et al. 2018; Yamazaki et al. 2017). Topographic data usually in the form

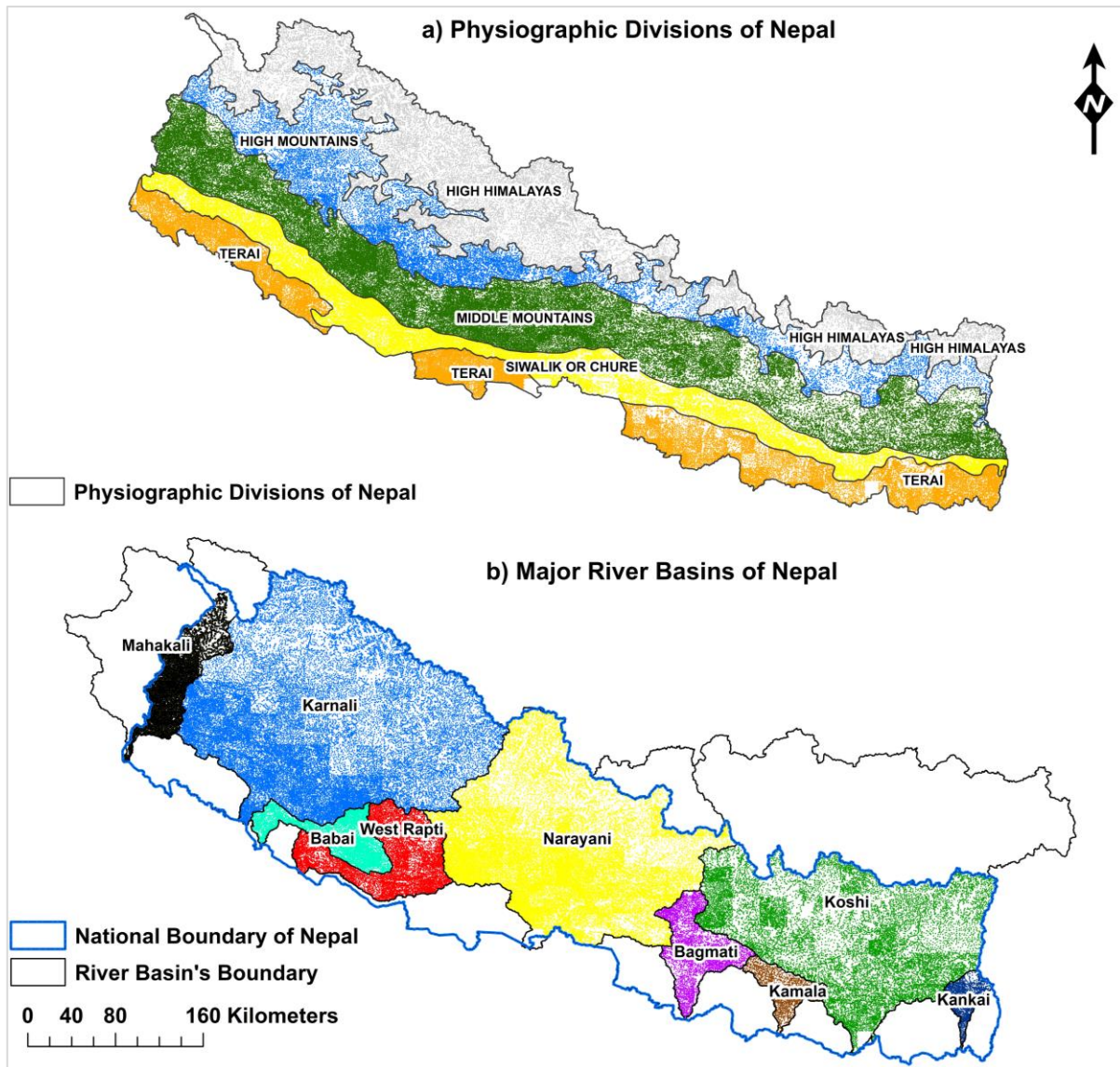
36 of DEMs are the most important input data in the study of different types of natural hazards
37 (Boreggio et al. 2018). Hydrologic and hydraulic tools entail the terrain data encompassing
38 from the reach to the basin scale. Delineation of catchment or watershed is carried out based on
39 DEMs which is a primary step for any geomorphological and hydrological studies. For instance,
40 popular hydrologic models like Soil and Water Assessment Tool (SWAT) (Winchell et al. 2013),
41 hydraulic models like Rainfall-Runoff-Inundation (RRI) model (Shrestha 2019), LIS-Flood
42 model (Coulthard et al. 2013), etc. all require DEMs or surface elevation as a primary dataset
43 for model set-up and simulation. Precise representation of the terrain is therefore vital for the
44 accurate prediction that closely agrees with the field observations. There are different
45 techniques which can be employed to generate high resolution digital terrain elevation maps.
46 High cost, time and sophisticated technology associated with these techniques renders them
47 difficult, if not impossible, for a large-scale application in a developing country with limited
48 resources. In the context of developing country like Nepal where the priorities that are centered
49 around the basic physical infrastructure and social development are yet to be achieved, mapping
50 and the preparation of high-resolution surface elevation is still far from the reality. Lack of high-
51 resolution topographical dataset is one of the major impediments to conduct research activities
52 across multiple fields in Nepal. A country with diverse landforms and elevation that ranges from
53 below 60m to the highest peak of the world (Mount Everest, at an elevation of 8848 meter above
54 sea level) in a mere 150Km-200Km stretch, the role of precise elevation dataset cannot be
55 overlooked. Schumann et al. (2018) has highlighted the growing need for the high resolution
56 DEMs. The availability of remotely sensed DEMs at varying spatial resolution have, however,
57 largely benefitted a nation like Nepal with lack of precise topography dataset. The problem
58 regarding the requirement of a country-scale high resolution topographic dataset has, to a certain
59 extent, been alleviated by these DEMs, if not completely. The analysis of different hydro-
60 climatic, environmental, geomorphological, etc. issues have been made possible by the
61 availability of multiple open access DEMs. The release of open access DEMs have eased the
62 analysis of global flood hazard at the global scale (Sampson et al. 2016).

63 In the midst of this, the problem pertaining to the accuracy of these products needs a proper
64 consideration. The assessment of the accuracy of DEMs is, therefore, a crucial step before
65 confirming their viability for any research studies or real field applications across different
66 fields. The availability of multiple DEMs, on one hand, has given greater access to the users
67 but at the same time it has also created a confusion among the users regarding the selection of
68 a particular DEMs for any applications. The DEMs, however, are not free from errors arising
69 from different sources during the observations and hence require prior processing. Several

70 analysis and application of the freely available DEMs such as the Shuttle Radar Topography
71 Mission (SRTM) or the Advanced Spaceborne Thermal Emission and Reflection Radiometer
72 (ASTER) have found to exhibit considerable error in vertical. Such errors are further aggravated
73 in the regions with diverse topography (Chu & Lindenschmidt 2017; Schumann et al. 2018).
74 Also, in the flat terrain, the topographic features are not well captured. The issue of the DEMs
75 accuracy has been addressed by several researchers. For instance, Pakoksung & Takagi (2016)
76 evaluated the accuracy of six different DEMs and hence applied the correction to minimize the
77 elevation bias. Their study revealed that the Root Mean Square Error (RMSE) value for coarser
78 resolution DEMs are higher than those of fine-resolution DEMs. Pakoksung & Takagi (2020)
79 also studied about the effect of DEMs on the prediction of run-off and inundation. Their analysis
80 revealed SRTM to perform better among ASTER, SRTM, GMTED2010, HYDROSHEDS, and
81 GTOPO30. In another study, Purinton & Bookhagen (2017) validated the accuracy of different
82 satellite-derived DEMs over Central Andean Plateau by comparing with GPS measurements.
83 They found the ASTER to be of the lowest quality except which all other selected DEMs had
84 the vertical accuracy below 4m.

85 Most of the previous studies, in general, have either evaluated the accuracy at a small region or
86 a single river basin (Mukherjee et al. 2012; Jing et al. 2014; Rawat et al. 2013). Similarly, the
87 accuracy assessment of DEMs in most cases has focused the evaluation at different elevation
88 bands of a river basin or a particular region. This may likely limit the assessment of the inherent
89 ability of the DEMs to accurately represent the diverse topographic features.

90 Unlike the aforementioned works, this study attempts to investigate the accuracy of eight freely
91 available DEMs across different physiographic regions as well as across major river basins of
92 Nepal. The main goal of our study is to investigate the performance and accuracy of different
93 space-borne DEM products, specifically across different physiographic regions and river basins
94 as explained above. There have been different studies regarding the accuracy assessment of
95 DEMs. However, this is the first assessment of the accuracy of open-source DEMs at a country-
96 scale in Nepal with diverse topography focusing different physiographic divisions and all the
97 major river basins. In the knowledge of the authors, so far, no formal validation of the accuracy
98 has been conducted for the recently released COPERNICUS DEM.



99

100 **Figure 1.** Physiographic divisions and major river basins of Nepal. The color inside the map
 101 indicates the reference points which is discussed in subsequent section.

102 **2. STUDY AREA**

103 Nepal is located between two large nations, China in the North while the southern part is
 104 bordered by India. Nepal is characterized by a diverse topographical and physiological
 105 landscape with variation in topography across a short North-South stretch. Its altitude ranges
 106 from less than 60m in the plains of southern Nepal to over 8000m (Mount Everest, the world's
 107 highest summit at elevation of 8,848 masl) in the north, within a short span of about 150 km,
 108 where the climate quickly changes from subtropical to arctic conditions (Dhital 2015).

109 As per the updated map released by the Survey Department in 2020, the area of Nepal is nearly
 110 148,000 square kilometers. Nepal is well-known around the world for the mountain ranges of

111 the Himalayas which includes 8 out of 14 peaks above 8000 meters in the world. The highest
112 peak of the world known as the Mount Everest (Sagarmatha in Nepalese language) also lies
113 within its territory. The world's deepest Kaligandaki gorge also lies here. The country is divided
114 into seven provincial units according to the constitution of Nepal.

115

116 **2.1 Physiographic divisions of Nepal**

117 Topographically, Nepal can be grouped into three distinct ecological divisions, Mountains, Hills
118 and Terai (or Plains), that extend throughout the east-west stretch of the country. Mountains in
119 the north lie at the highest elevation range followed by the Hills and the Terai in the southern
120 part. The broad and widely adopted physiographic units of Nepal, however, comprise of five
121 major divisions viz. high himalayas, high mountains, middle mountains, siwalik (or chure) and
122 the Terai (**Figure 1a**). Each of these physiographic units are characterized by its unique
123 topographical, climatic and vegetational features (Upreti 2001). According to Hagen (1969),
124 the currently adopted five physiographic classes has further been divided into eight
125 physiographic units (Upreti 2001).

126 Terai, the southern unit bordering with India forms the northernmost part of the Indo-Gangetic
127 plain. Along the north, it extends to the foothills of the Siwalik that varies in width
128 approximately between 10km to 50km. Except for about 70Km span of Chitwan valley at the
129 central part and 80Km of the Rapti valley in the west, the Terai region forms continuous belt
130 from the east to the west (**Figure 1a**). At these two locations, the Indo-Nepal border meets the
131 Siwalik. The elevation normally ranges between 100-200m.

132 At the end of the Terai in the north, the abrupt rise in the topography occurs which is the
133 beginning of the Siwalik. The Siwalik hills are often referred as the Chure range in Nepal which
134 occupies about 13% of the total area of Nepal. It forms the southernmost hills of the Himalayas.
135 The elevation generally varies between 200masl to 1000masl and reaches even higher in some
136 locations. Characterized by young and immature geology, these hills are the most fragile in
137 terms of geomorphological features. Numerous gullies and channels dissect these hills which
138 carries significant sediment as a result of the soil erosion and landslides. The rivers originating
139 from these hills are generally ephemeral in nature exhibiting river flow only during the monsoon
140 period. From the view point of conservation, the Siwalik region comes in the top priority be its
141 forest, land resources, rivers, etc.

142 Middle mountains, also known as the Mahabharat range, is the largest physiographic unit of
143 Nepal covering nearly 30% of the total area of the country. The Middle Mountain area

144 comprises the country's central belt which is composed of networks of ridges and incised
145 valleys (Bricker et al. 2014). High Mountains and High Himalayas which are the source of the
146 major rivers of Nepal comprises almost half of the total area of Nepal. However, due to extreme
147 topographical and climatic features, these regions are one of the least populated area of Nepal.

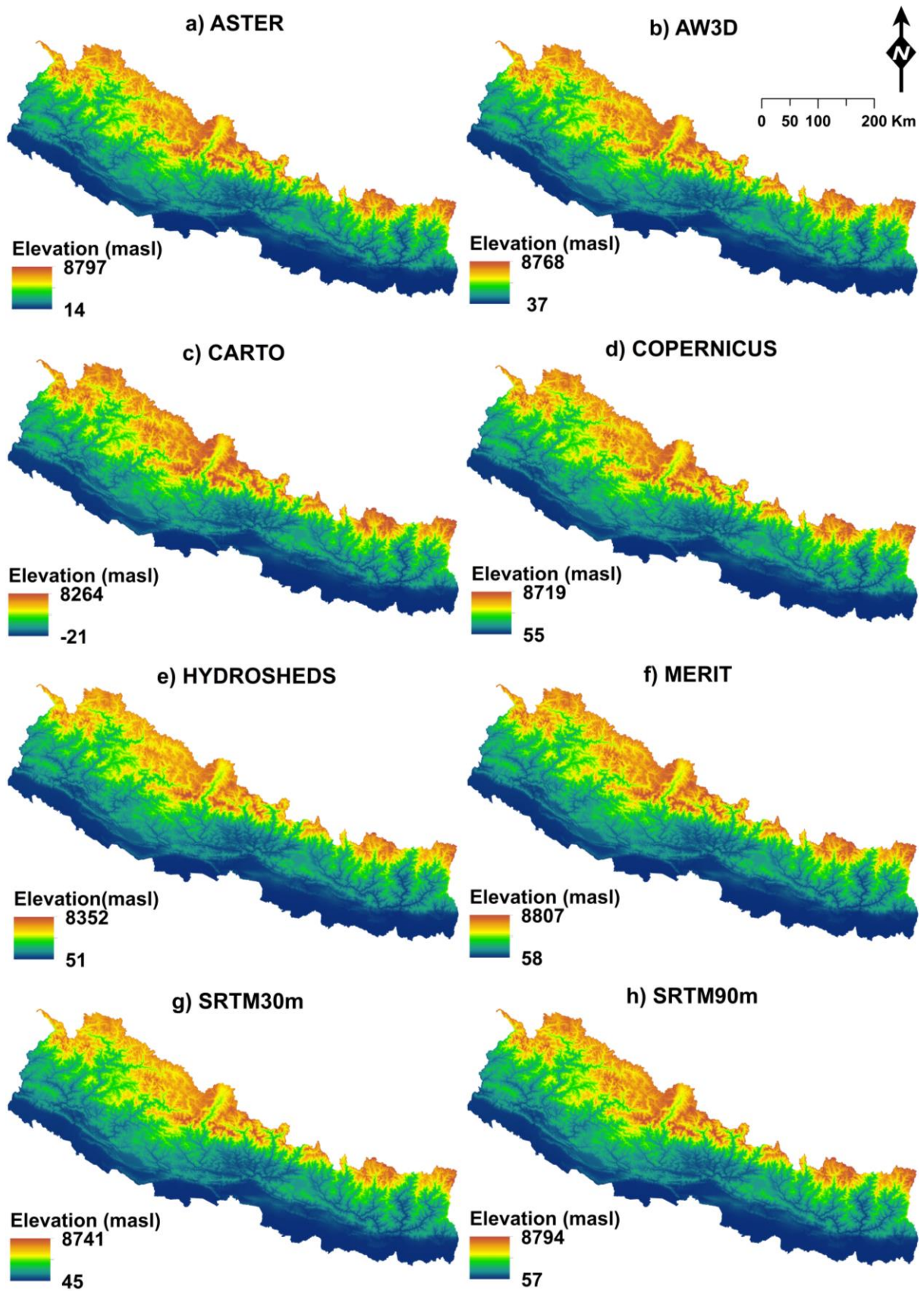
148 **2.2 River systems of Nepal**

149 The river basins of Nepal can be broadly divided into four major systems, Koshi (or Saptakoshi)
150 in the east, Narayani (or Gandaki) in the central, Karnali in the west and Mahakali in the far
151 west (**Figure 1b**). Out of these, the three Koshi, Narayani and Karnali originate from the Tibetan
152 plateau and cross the Himalayas (Sharma 1987). The flow in these Himalayan rivers is governed
153 by the snowmelt and the glaciers. Apart from these, another group comprise of the rivers
154 originating in the middle mountains whose flow regimes are dictated by the rainfall and the
155 groundwater that prevents the rivers from being completely dry during the low flow period.
156 Kankai, Kamala, Bagmati, West Rapti and Babai are few examples under this group. These
157 rivers have high fluctuations in the discharge between the dry period and the monsoon period.
158 The third group of rivers originate in the Siwalik zone. The flow in these rivers is mostly
159 dependent on monsoon precipitation and their flow level could deplete significantly low during
160 the non-monsoon period. In Nepal, approximately six thousand minor and major streams that
161 span over 40000Km carry annual flow volume of about 1.7billion cubic meters (DoWRI 2019).
162 The drainage density of Nepal (total river length divided by the total area) is close to
163 0.3km/square km. The entire area of Nepal forms part of the watershed of Ganges and hence all
164 the Rivers from Nepal eventually join Ganges in India. The Nepalese Rivers contribute as much
165 as 40% flow of Ganges in monsoon and about 70% flow in dry period.

166 In this study, the four major Himalayan River basins, Koshi, Narayani, Karnali and Mahakali
167 and the five river basins originating in the middle mountains, Kankai, Kamala, Bagmati, West
168 Rapti and Babai are considered (**Figure 1b**). These rivers are characterized by single thread
169 high gradients channels (with frequent meanders) with catchments comprising of steep terrain
170 in the upper reach. The river gradient significantly decreases towards the Terai plain in south.
171 The rivers in the Terai plains are usually braided in nature having multiple channels and often
172 changes the course. The elevation range within each basin are therefore wide that varies in few
173 hundreds to few thousand meters.

174 **3. MATERIALS AND METHODS**

175



176

177 **Figure 2.** Elevation of Nepal as represented by different DEMs.

178 **3.1 Digital Elevation Models**

179 In this study, eight different freely available DEMs are examined for their vertical accuracy.
 180 **Figure 1(a-h)** exhibit the elevation distribution of different DEMs across the country. **Table 1**
 181 lists the general information regarding the characteristics of these DEMs including their source,
 182 resolution, release year, etc.

183

184 **Table 1.** Characteristics of the DEMs used in this study

| DEM | Resolution | Originally Release year | Source | Version used in this study | Elevation Range for Nepal (Min/Max) masl |
|-------------------|------------|-------------------------|----------------------------|----------------------------|--|
| ASTER | 30m | 2019 | METI/NASA | ASTGTMV003 | 8797/14 |
| AW3D | 30m | 2016 | JAXA | 3.1 | 8768/37 |
| CARTO | 30m | 2005 | ISRO | 3-R1 | 8226/-21 |
| COPERNICUS | 30m | 2019 | ESA | GLO-30 | 8719/55 |
| HYDROSHEDS | 90m | 2009 | WWF/USGS | | 8315/60 |
| MERIT | 90m | 2017 | University of Tokyo, Japan | v1.0.3 | 8807/58 |
| SRTM30m | 30m | 2014 | NASA/USGS | 3.0 | 8741/45 |
| SRTM90m | 90m | 2003 | NASA/USGS | 4.1 | 8794/57 |

185

186 The Advanced Space borne Thermal Emission and Reflection Radiometer (ASTER) Global
 187 Digital Elevation Model (GDEM) is the product of joint mission of the United States National
 188 Aeronautics and Space Administration (NASA) and the Ministry of Economy, Trade, and
 189 Industry (METI) of Japan (Toutin 2008; Gesch et al. 2016) . ASTER DEM has been developed
 190 from ASTER scenes dating from March 1, 2000 to November 30, 2013 whose geographic
 191 coverage extends from 83° North to 83° South at the horizontal resolution of 30m. ASTER
 192 Global Digital Elevation Model V003 has been used in this study which was obtained from the
 193 Land Processes Distributed Active Archive Center (LP DAAC) via NASA’s Earthdata search
 194 (<https://search.earthdata.nasa.gov/>).

195 Advanced Land Observing Satellite (ALOS) World 3D-30m (AW3D30) DEM has been
 196 released by The Japan Aerospace Exploration Agency (JAXA) in 2016 (Nikolakopoulos 2020).
 197 AW3D is a global digital surface model (DSM) dataset with a horizontal resolution of
 198 approximately 30 meters (1 arcsec mesh). The dataset is based on the DSM dataset (5-meter
 199 mesh version) of the World 3D Topographic Data (JAXA 2017). The AW3D DEM was
 200 generated by the “Panchromatic Remote-sensing Instrument for Stereo Mapping (PRISM)” on
 201 the “Advanced Land Observing Satellite (ALOS)” which operated from January 2006 to April

202 2011 (Takaku et al. 2016; Yamazaki et al. 2017). Version 3.1 datasets were acquired from the
203 official website of ALOS Research and Application project.

204 (<https://www.eorc.jaxa.jp/ALOS/en/aw3d30/data/index.htm>)

205 The Cartosat-1 Digital Elevation Model (CartoDEM) is a national DEM developed by the
206 Indian Space Research Organization (ISRO) which is derived from the Cartosat-1 stereo
207 payload launched in May 2005 (Mukherjee et al. 2012). For this study, CartoDEM Version-3R1
208 was downloaded from the bhuvan, Indian geo-platform of ISRO ([https://bhuvan-
209 app3.nrsc.gov.in/data/](https://bhuvan-app3.nrsc.gov.in/data/)). The data for Nepal is available at the horizontal resolution of 30m.

210 The Copernicus DEM has been derived from the WorldDEM data which is based on the radar
211 satellite data acquired during the TanDEM-X Mission between 2010-2015, funded by a Public
212 Private Partnership between the German State, represented by the German Aerospace Centre
213 (DLR) and Airbus Defence and Space (Leister-Taylor 2020). The Copernicus DEM is provided
214 in 3 different forms viz. EEA-10, GLO-30 and GLO-90. In the current study, GLO-30 available
215 at 30m horizontal resolution was acquired from the European Space Agency Copernicus
216 website (<https://panda.copernicus.eu/web/cds-catalogue/panda>).

217 HydroSHEDS (Hydrological data and maps based on SHuttle Elevation Derivatives at multiple
218 Scales) DEM is derived primarily from elevation data of the Shuttle Radar Topography Mission
219 (SRTM) at 3 arc-second (90m) resolution by hydrological conditioning using a sequence of
220 automated procedures (Lehner et al. 2013; Yan et al. 2019). HydroSHEDS data can for this
221 study was downloaded from <https://www.hydrosheds.org/>

222 The MERIT DEM, regarded as one of the most accurate global DEMs, was developed by the
223 group of researchers from the University of Tokyo, Japan. It removed characteristic errors
224 found in these products that included: stripe noise, absolute bias, tree height bias and speckle
225 noise from the existing spaceborne DEMs (SRTM3 v2.1 and AW3D-30m v1) (Yamazaki et al.
226 2019; Amatulli et al. 2020). It is available at a 3sec resolution (~90m at the equator) and the
227 spatial coverage includes land areas between 90N-60S, referenced to EGM96 geoid (Yamazaki
228 et al. 2017). Merit DEM can be acquired via

229 http://hydro.iis.u-tokyo.ac.jp/~yamada/MERIT_DEM/

230 Shuttle Radar Topography Mission (SRTM), a joint mission of National Imagery and Mapping
231 Agency (NIMA) and NASA produced one of the first global DEMs that was first released with
232 a spatial resolution of 3 arc-second (Bhang et al. 2007; Farr et al. 2007; SRTM 2015). SRTM
233 consisted of a specially modified radar system that flew onboard the Space Shuttle Endeavour
234 during an 11-day mission between February 11-22, 2000 (Ling et al. 2005). In 2014, its 1 arc-s
235 global digital elevation model (~30 m) was released. Most parts of the world have been covered

236 by this data set, ranging from 54°S to 60°N latitude, except for the Middle East and North Africa,
 237 which was completed in August 2015 (Nadi et al. 2020). The updated 30m DEM has been
 238 released recently to include coverage over Asia and Australia (NASA 2013). The data were
 239 downloaded from the LP DAAC via NASA's Earthdata search
 240 (<https://search.earthdata.nasa.gov/>).

241

242 3.2 Reference Elevation data

243 The assessment of the accuracy of DEM requires reference elevation data which are based on
 244 the ground observation having higher reliability than the DEM elevations (Pakoksung & Takagi
 245 2016). To this end, we acquired the spot elevation (surveyed elevation point marked from the
 246 DoS Toposheet) dataset of more than 120000 points covering the whole country from the
 247 Department of Survey (DoS), Nepal. DoS is the national mapping agency of Nepal that is
 248 primarily responsible for the surveying, mapping, geoinformation science and earth observation
 249 (DoS 2021; Baral 2006). Spot elevation are the digital point data of elevation point locations of
 250 Nepal which are based on the Topographic Zonal Map of 250000 scale published by DoS, Nepal
 251 in 1988. During the period between 1992 to 2001, DoS updated the old data with a completely
 252 new series of topographic base maps replacing the old one inch to one-mile maps. These maps
 253 were produced at a scale of 1:25,000 for the terai and the middle mountains; and at a scale of
 254 1:50,000 for the high mountains and Himalayas (Chhatkuli 2003). The spatial distribution of
 255 spot elevation point data at the physiographic level and the river basin level is depicted in
 256 **Figure 1a** and **b**. The details on these datasets at each physiographic region and the river basin
 257 level are listed in **Table 2** and **3** respectively.

258

259 **Table 2.** Details on the data points across the physiographic units.

| Physiographic Divisions | Area (Sq. Km.) | Percentage of area occupied | No. of Spot elevations points | Density of points | Elevation Range (Min/Max) masl |
|---------------------------|----------------|-----------------------------|-------------------------------|-------------------|--------------------------------|
| Terai | 20217 | 14 | 22533 | 1.115 | 59/721 |
| Siwalik (or Chure) | 18976 | 13 | 21078 | 1.111 | 92/1972 |
| Middle Mountains | 43079 | 29 | 45634 | 1.059 | 152/3452 |
| High Mountains | 30103 | 20 | 15593 | 0.518 | 515/5202 |
| High Himalayas | 35353 | 24 | 15673 | 0.443 | 2150/8749 |

260

261

262 **Table 3.** Details on the data points across the river basin units.

| River Basins | Total Area (Sq. Km.) | Area within Nepal (Sq. Km.) | Percentage of area in Nepal (%) | No. of Spot Elevation Points | Point Density (Points per Sq. Km) | Elevation Range (Min/Max) masl |
|-------------------|----------------------|-----------------------------|---------------------------------|------------------------------|-----------------------------------|--------------------------------|
| Kankai | 1280 | 1280 | 100 | 1504 | 1.2 | 76/3234 |
| Koshi | 59565 | 27687 | 46 | 14676 | 0.5 | 66/8586 |
| Kamala | 2007 | 2007 | 100 | 1507 | 0.8 | 68/2021 |
| Bagmati | 4304 | 4304 | 100 | 3339 | 0.8 | 71/2697 |
| Narayani | 36598 | 32094 | 88 | 26316 | 0.8 | 110/8167 |
| West Rapti | 6449 | 6444 | 100 | 8224 | 1.3 | 131/3267 |
| Babai | 3424 | 3424 | 100 | 5096 | 1.5 | 138/2445 |
| Karnali | 45974 | 42909 | 93 | 29324 | 0.7 | 137/7751 |
| Mahakali | 15460 | 5209 | 34 | 4669 | 0.9 | 154/7132 |

263

264 3.3 Methodology

265 The overall methodology in this study involves the use of ArcGIS, excel and python tools. The
 266 point shapefile of the spot elevation data along with the layers of physiographic and river basins
 267 divisions were imported in the ArcMap platform of ArcGIS. These points lying within each
 268 physiographic unit were separately clipped and the DEM elevation at these point locations were
 269 extracted using ‘Extract Multi values to Points’ tool within spatial analyst toolbox in ArcMap.
 270 This resulted in a separate elevation field for each of the DEM used, corresponding to the spot
 271 elevation points. The attributes were then exported to excel for further analysis. The same
 272 procedure was followed for the analysis at the river basin level too.

273 The accuracy was evaluated based on some commonly adopted statistical measurements (**Table**
 274 **4**). The vertical accuracy of the eight DEMs used in this study was calculated from the
 275 differences corresponding between the elevation of the DEM pixel and the reference point spot
 276 elevation. Elevation error (the difference in elevation between DEM and spot elevation,
 277 $(Z_{Error} = Z_{DEM} - Z_{SEI})$) was estimated where the positive error denote overestimation in DEM
 278 while the negative error denotes underestimation of DEM elevation. The mean of the reference
 279 spot elevation and the DEM elevation over each physiographic division (or river basins) was
 280 calculated as the sum of the elevation divided by the number of points. The other statistics
 281 (**Table 4**) mean error (ME), mean absolute error (MAE), root mean square error (RMSE) were
 282 calculated based on the elevation error as described above. Additionally, the coefficient of
 283 determination (R^2) between spot elevation and each of the DEMs elevation was also assessed
 284 separately for each physiographic division and river basin. A histogram of the mean error of
 285 each DEM for each of the physiographic unit (and river basin) was plotted. A normal

286 distribution curve was fitted to the histogram. Finally based on each of the statistical
 287 measurements, the ranking of the DEMs was evaluated.

288

289 **Table 4.** Statistical measurement adopted for the evaluation of accuracy of DEMs.

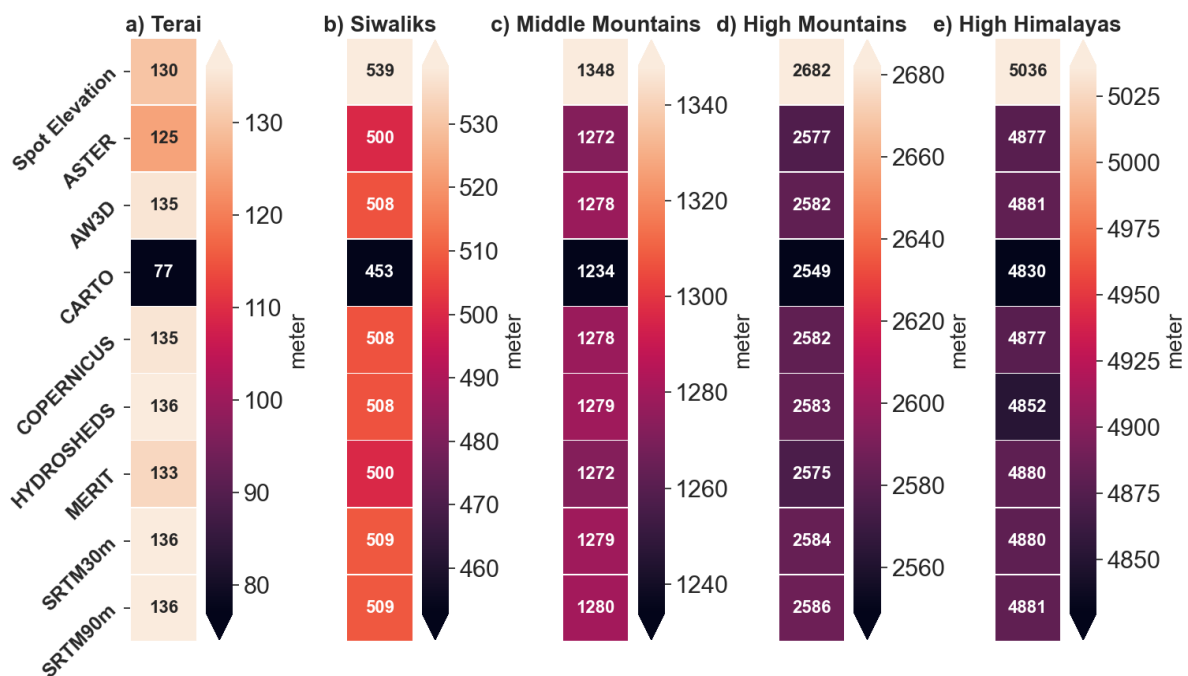
| Error Statistics | Description |
|-------------------------------|--|
| Elevation Error | $Z_{error} = Z_{DEM} - Z_{SEL}$ |
| Mean Error (ME) | $ME = \frac{\sum_{i=1}^n Z_{error}}{n}$ |
| Mean Absolute Error (MAE) | $MAE = \frac{\sum_{i=1}^n Z_{error} }{n}$ |
| Root Mean Square Error (RMSE) | $\sqrt{\frac{\sum_{i=1}^n (Z_{error(i)})^2}{n}}$ |

290 **4. RESULTS AND DISCUSSION**

291 The results for the physiographic and river basin level are discussed separately.

292 **4.1 Evaluation across the physiographic unit**

293 The analysis of the results across the physiographic divisions are presented herein.

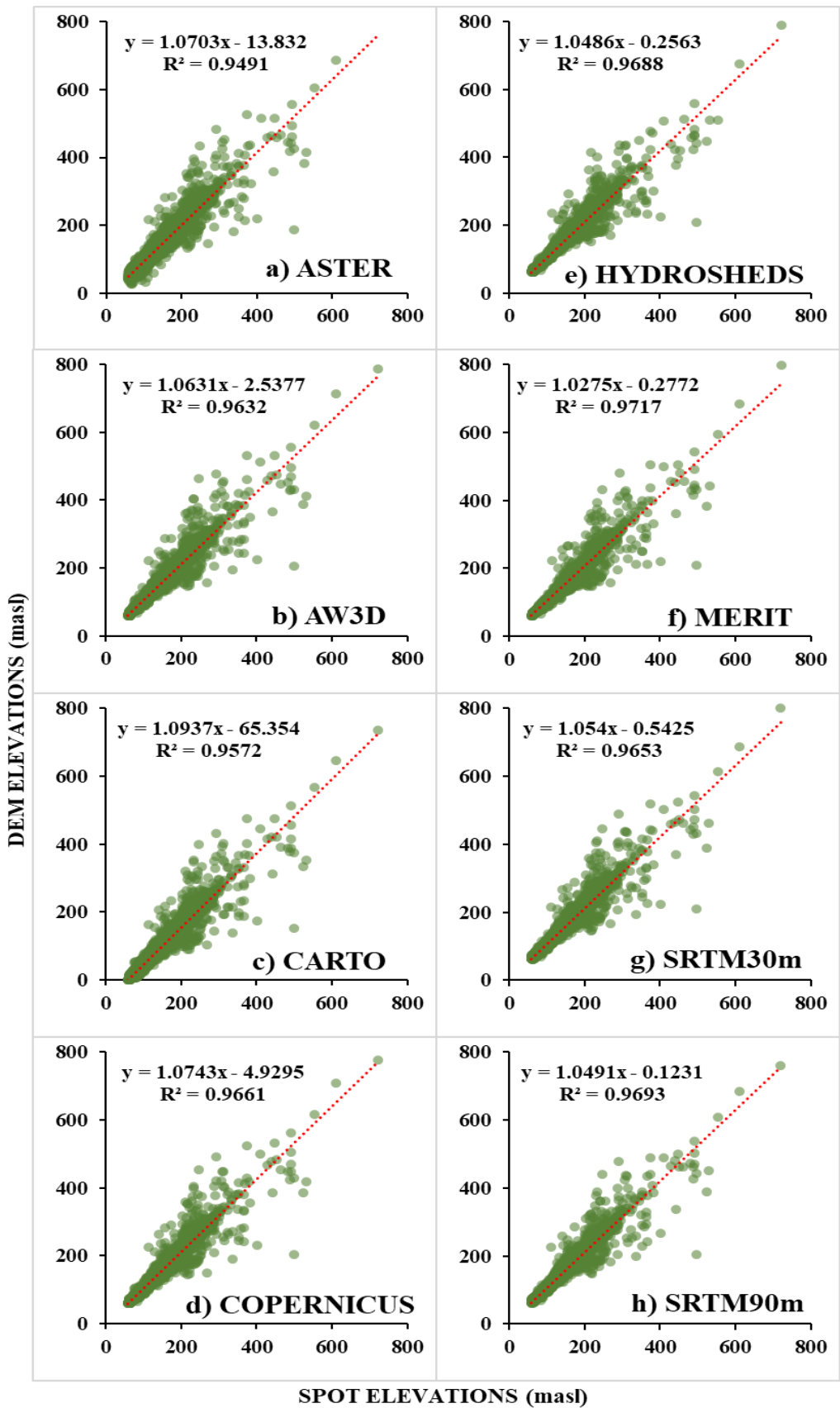


294

295 **Figure 4.** Comparison of the mean value of reference spot elevation data with different DEMs
 296 elevation for each physiographic unit.

297 The mean of the spot elevation points within each physiographic unit and the mean of the DEMs

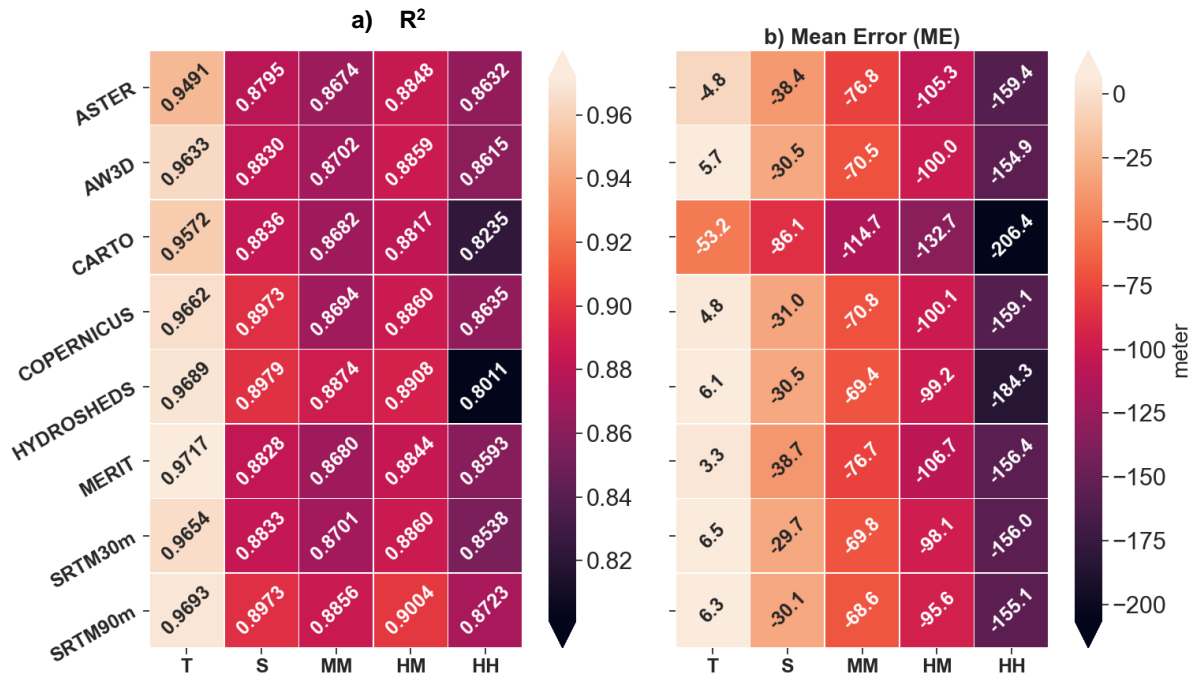
298 elevation corresponding to these points were compared (**Figure 4a-e**). Except for the Terai, the
299 mean elevation of each of the DEMs showed underestimation across every physiographic
300 division. Carto DEM showed the maximum underestimation at every physiographic unit while
301 in Terai the ASTER DEM also displayed a slight underestimation (-5m). Apart from these, in
302 Terai, all other six DEMs exhibited overestimation ranging from +3m to +6m. MERIT DEM
303 with an overestimation of +3m depicted better performance among all others (**Figure 4a**). Terai
304 being the southern plain are the most prone to floods, sedimentation and inundation problems
305 as all the rivers from the north traverse this region. The elevation ranges also being
306 comparatively narrower in Terai due to the flat area, the accuracy of DEM is highly necessitated
307 for their application in any works related to the landuse planning and management, floods
308 management, etc. In this regard, Japan International cooperation agency (JICA) is analyzing the
309 viability of preparing a high resolution DEM of 13 districts in Terai of Province 1 and 2 and 3
310 (JICA 2020).



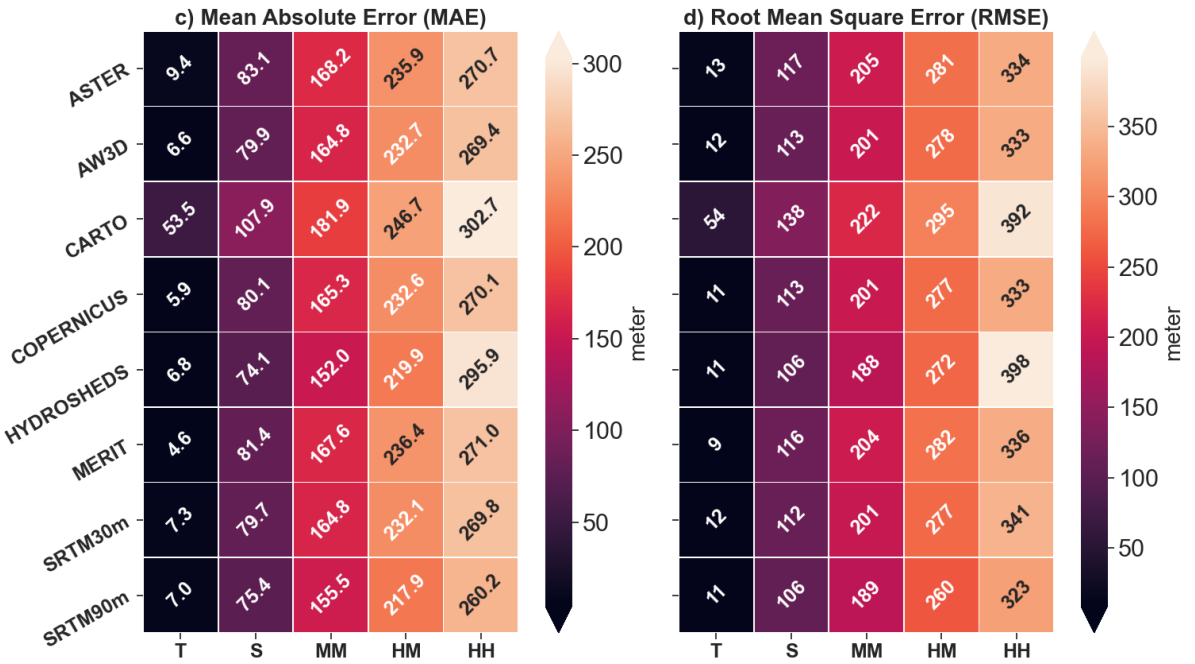
311

312 **Figure 5.** Scatterplot of reference spot elevation versus elevation of different DEMs at
 313 corresponding points for the Terai region.

314



315



316

[T: Terai S: Siwalik MM: Middle Mountains HM: High Mountains HH: High Himalayas]

317

Figure 6. Comparison of different statistical measurement for each DEMs estimated from the elevation error across each physiographic unit.

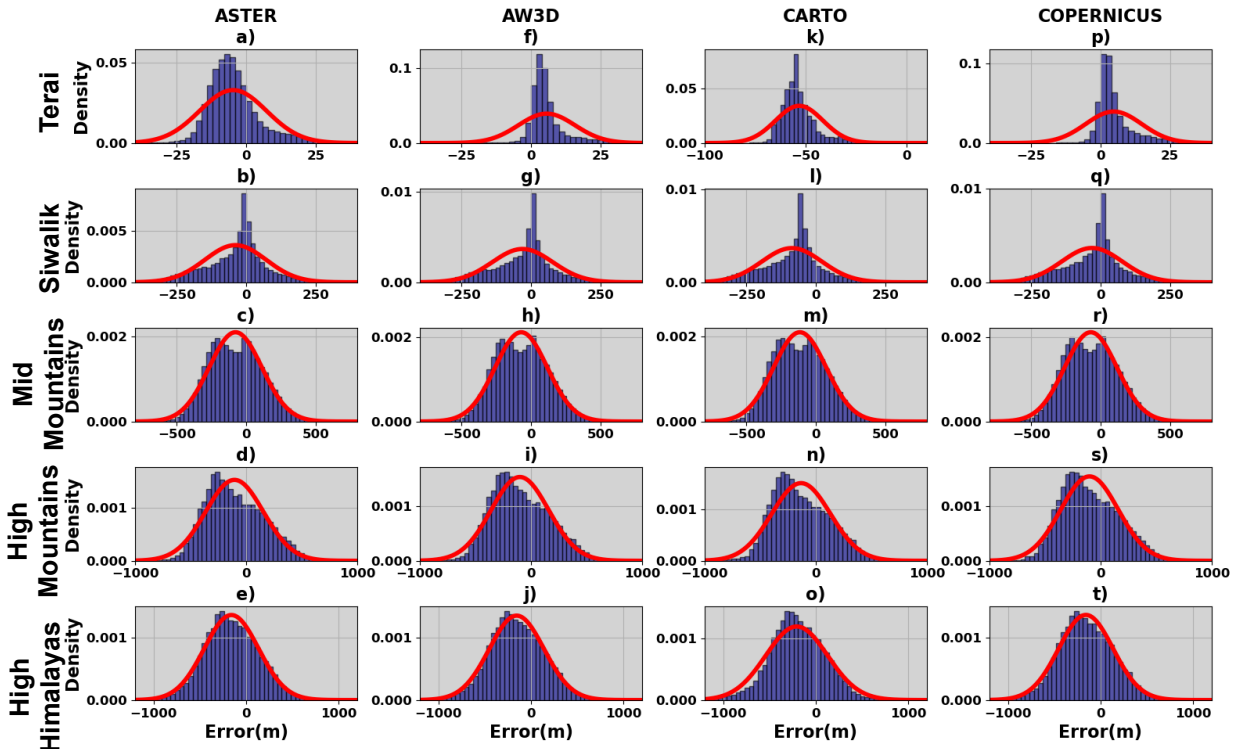
319

The deviation of the DEMs elevation from the reference spot elevation is given by mean error (ME) in **Figure 6b**. In Siwalik region, ASTER and MERIT, showed greater deviation (both above -38m) after CARTO while the remaining SRTM30m, SRTM90m, HYDROSHEDS, COPERNICUS and AW3D showed almost similar results (error approximately between -30m to -31m) (**Figure 6b**). Except CARTO, the mean error of other DEMs for MM, HM and HH

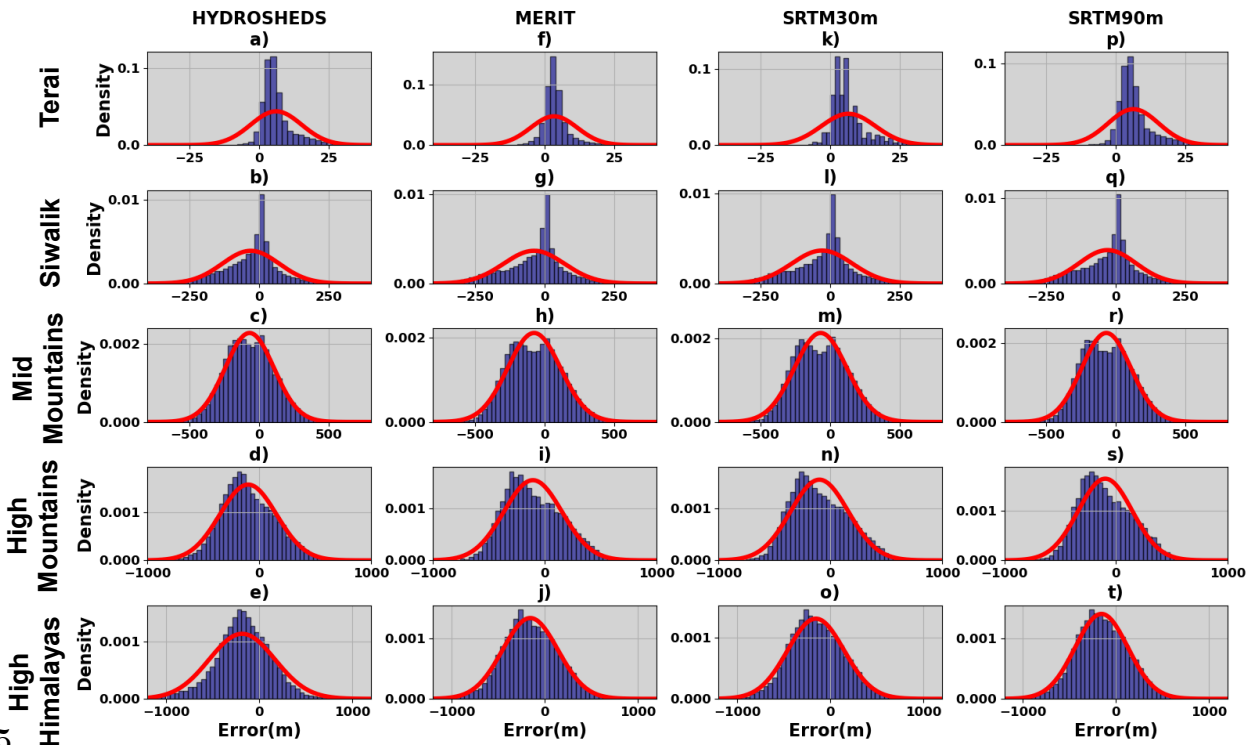
323

324 was in the range of -68.6m to -76.8m, -95.6m to -106.7m and -154.9m to -184.3m respectively.
325 The correlation plot between the spot elevation points and the DEMs elevation at corresponding
326 points for the Terai region is illustrated in **Figure 5a-h**. But the coefficient of determination
327 (R^2) values between spot elevation and each DEMs across every physiographic division is
328 depicted in **Figure 6a**. In general, the R^2 values were excellent for each DEMs and across every
329 division. Nevertheless, the values were higher (>0.9491) for Terai while for S, MM and HM,
330 the values were very close to each other (from 0.87 to slightly above 0.90). Meanwhile, the
331 correlation was relatively lower for High Himalayas (**Figure 6a**) which is likely due to the
332 smaller number of elevation points with comparison to others. Likewise, MAE and RMSE are
333 portrayed in **Figure 6c-d** respectively. The values of MAE and RMSE for each DEMs across
334 each physiographic division followed the same pattern as of mean error. Since the elevation
335 range increases from the south to the north, the error range also followed the same pattern.
336 Analysis by Mukherjee et al. (2012) also showed the DEM elevation to be more erroneous in
337 high altitudinal zone where terrain is rugged.

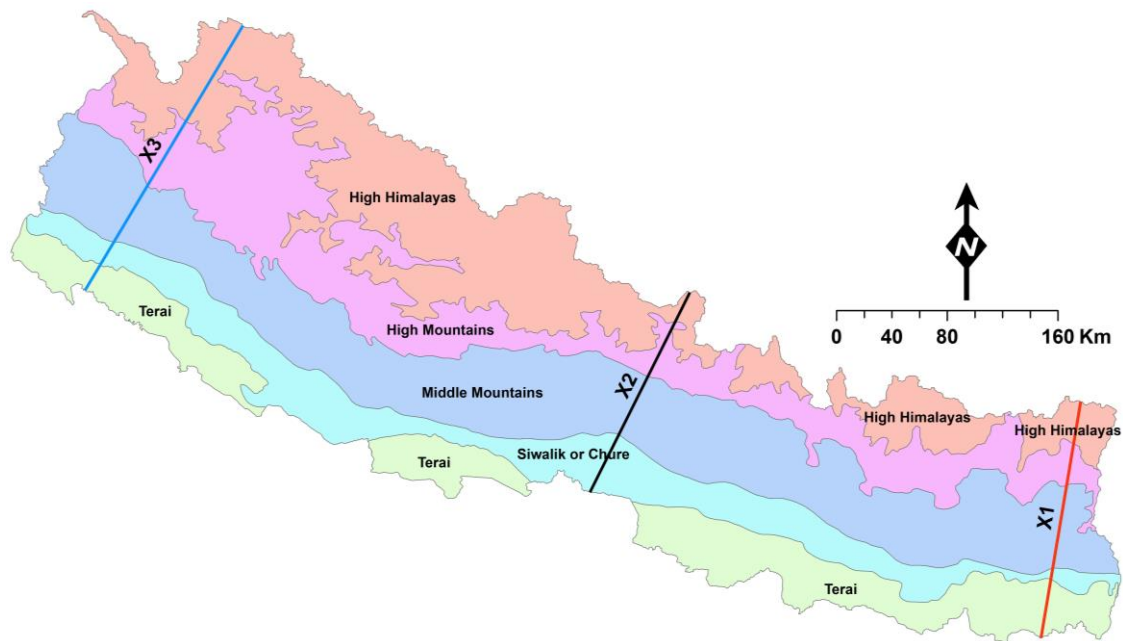
338 **Figure 7** and **8** illustrate the histogram of elevation errors for each DEM across different
339 physiographic division. The normal distribution curve is fitted to the elevation errors which is
340 represented by the bold red line in all the graphs. The histogram plot clearly shows that the
341 negative bias is dominant in almost all of the DEMs across all physiographic division indicating
342 underestimation of the DEMs elevation. The histogram, in general, revealed that the frequencies
343 of negative errors are higher than the positive ones. This meant that the frequencies of the
344 negative errors are positively skewed. However, in the case of Terai, all DEMs except ASTER
345 and CARTO indicated the frequency of positive error to be greater than the negative ones which
346 implied that the frequency of positive errors is negatively skewed. The mean error for these two
347 DEMs are therefore negative (-4.8m for ASTER and -53.2m for CARTO). The histogram of
348 AW3D, COPERNICUS, HYDROSHEDS, MERIT, SRTM30m and SRTM90m all displayed a
349 bias toward positive values on a normal distribution and hence the mean error for these six
350 DEMs revealed positive values in the Terai.



351
 352 **Figure 7.** Histogram of elevation error for ASTER, AW3D, CARTO and COPERNICUS across
 353 each physiographic division. The red line in the figure represents the fitted curve based on
 354 normal distribution.



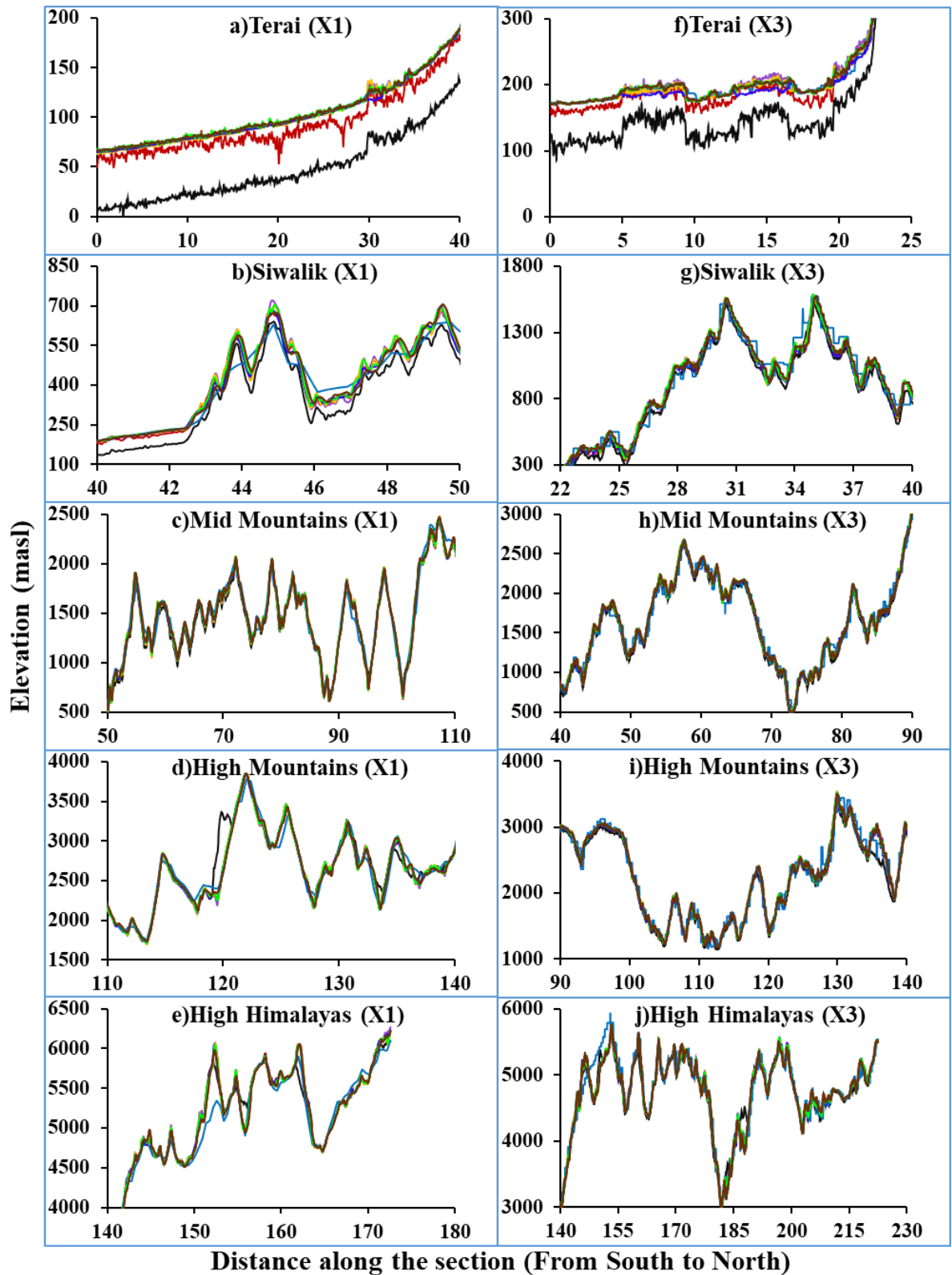
355
 356 **Figure 8.** Histogram of elevation error for HYDROSHEDS, MERIT, SRTM30m and
 357 SRTM90m across each physiographic division. The red line in the figure represents the fitted
 358 curve based on normal distribution.



359

360 **Figure 9.** Physiographic Divisions with three arbitrary cross-section lines for plotting
 361 elevation profiles.

362 Three arbitrary cross-sections, one at the eastern part, second at the central part and the last at
 363 the western part, were drawn along the south-north direction of the country (**Figure 9**). Points
 364 were generated along these cross-section lines at an interval of 30m. DEMs elevation at these
 365 points along each cross-section are plotted against the cumulative distance (in kilometer)
 366 beginning from the south (**Figure 10a-j** and **Figure 11a-d**). In MM and HM, the elevation of
 367 each DEMs nearly matched each other (**Figure 10c-d, h-i** and **Figure 11b-c**). However, in the
 368 case of Terai, the elevation of CARTO was highly below the other DEMs showing consistent
 369 downward shift. The elevation of ASTER too was below the other DEMs but having relatively
 370 lower difference than the CARTO. The other DEMs, however, showed almost similar elevation
 371 trend. It can be observed that the elevation drops by over 150m at a distance of about 40Km at
 372 X1 (**Figure 10a**) and more than 100m at a distance of 22Km at X3 (**Figure 10f**). In Siwalik
 373 region, the elevation of CARTO was again below other DEMs particularly around the valley
 374 areas (**Figure 10b** and **11a**) while the HYDROSHEDS elevation was slightly above others
 375 around the valley of Siwalik region. At X2, the Siwalik hills form the border with India,
 376 therefore the Terai is missing in **Figure 11**.



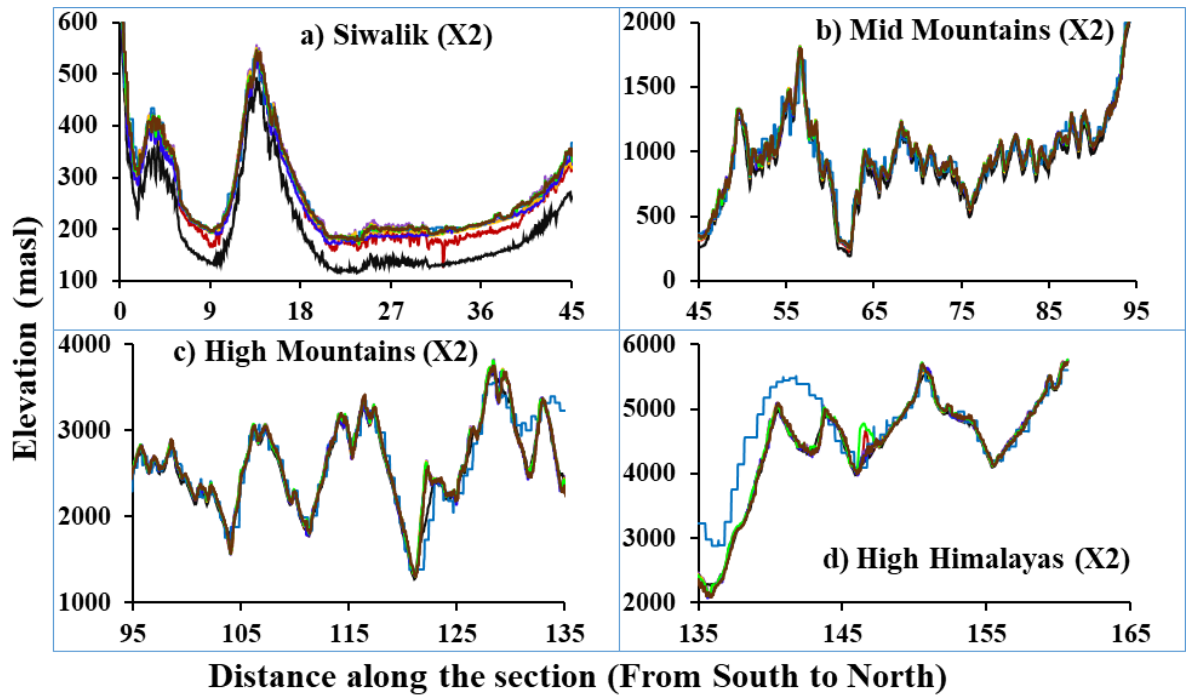
377



378

379 **Figure 10.** Elevation of different DEMs along the cross-section X1 and X3 as indicated in

380 **Figure 9** for different physiographic division.



381

382

383 **Figure 11.** Elevation of different DEMs along the cross-section X2 as indicated in **Figure 9**

384 for different physiographic division.

385

386

387

388

389

390

391

392

393

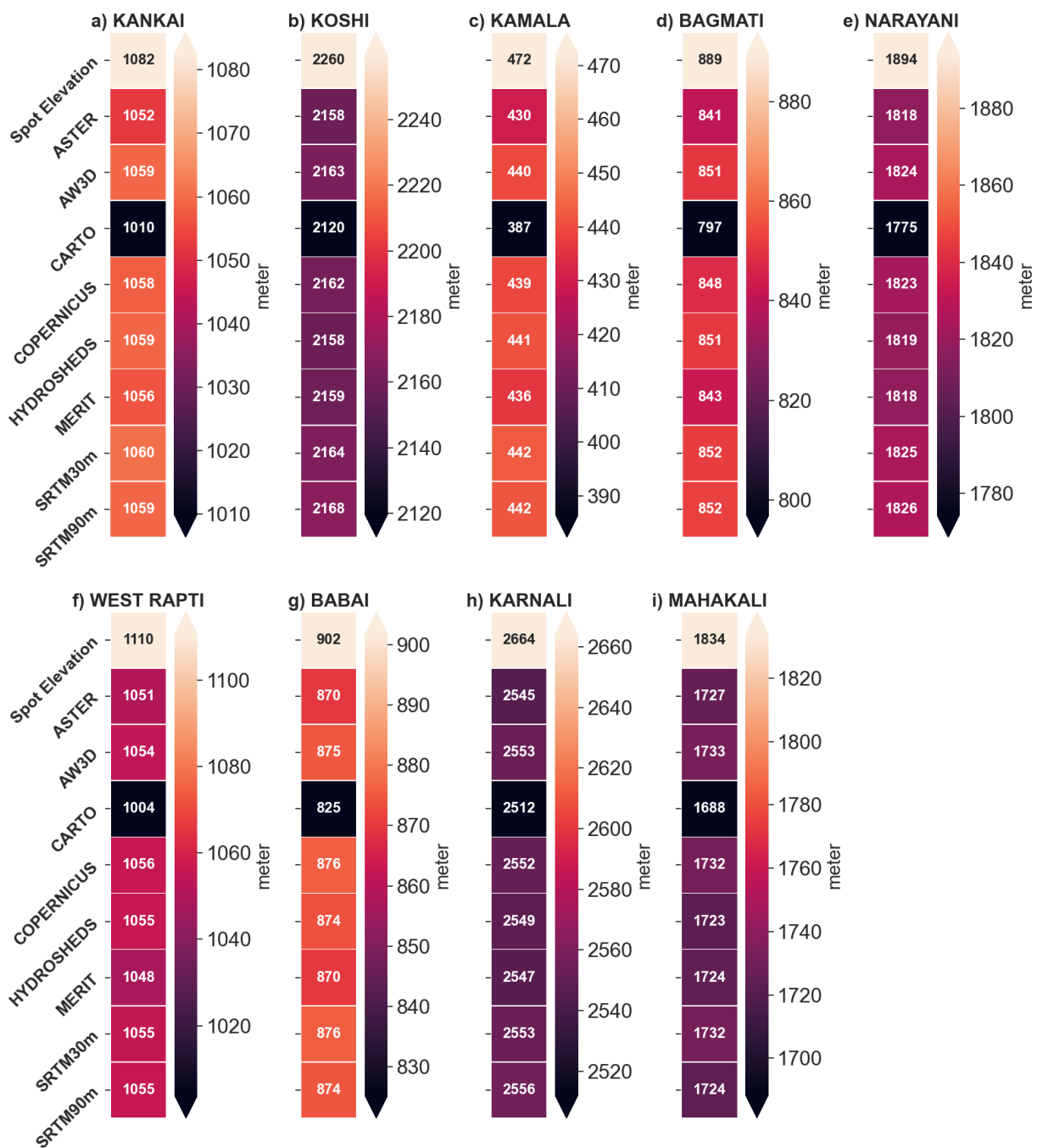
394

395

396

397 **4.2 Evaluation across the river basins**

398 The analysis of the accuracy of DEMs across the river basins are presented in a similar way to
 399 the analysis across the physiographic divisions

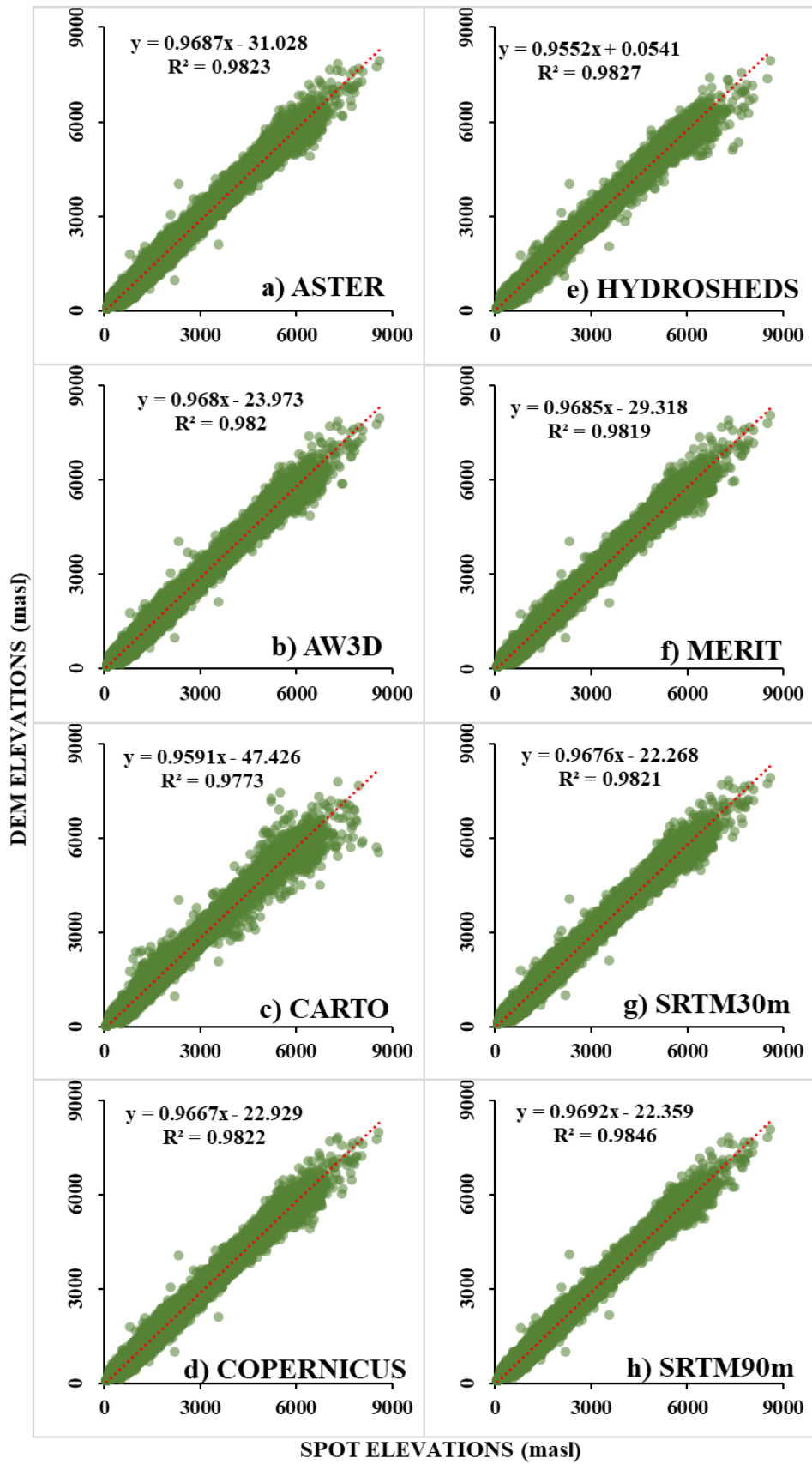


401
 402 **Figure 12.** Comparison of the mean value of reference spot elevation data with different DEMs
 403 elevation for each river basins.
 404 The mean of the spot elevation points within each river basin and the mean of the DEMs
 405 elevation corresponding to these points were compared (**Figure 12**). Each DEMs across all the
 406 river basins showed underestimated elevation compared to the spot elevation mean. As in the

407 case of physiographic divisions, CARTO displayed the maximum underestimation from the spot
408 elevation mean in each river basins. After CARTO, the ASTER depicted greater
409 underestimation in all basins except West Rapti and Mahakali.

410 The estimation of different error statistics is presented in **Figure 14a-d**. The R^2 value in general
411 were in a good range for all the DEMs (**Figure 14a**). Nevertheless, larger basins like Koshi,
412 Narayani, Karnali relatively displayed higher R^2 (>0.98). In general, the elevation of SRTM90m
413 better correlated with the spot elevation in each river basins. The correlation plot of spot
414 elevation points versus DEMs elevation for the Koshi river basin also depicts higher R^2 (0.9846)
415 for SRTM90m (**Figure 13**). The range of the elevation is also higher in Koshi basin among all
416 other river basins (**Figure 3** and **Table 3**). Meanwhile, SRTM90m also discerned the minimum
417 mean error for four of the river basins including Koshi (-90m), Bagmati (-37m), Narayani (-
418 68m) and Karnali (-109m) (**Figure 14b**). For other basins (Kankai, Kamala, Babai and
419 Mahakali), SRTM30m revealed the minimum mean error (-22m, -30m, -26m and -102m
420 respectively). Similarly, the mean error estimated for COPERNICUS was the minimum (-55m)
421 in West Rapti basin in comparison to the other DEMs. In Mahakali basin, AW3D and
422 COPERNICUS and in Babai, COPERNICUS also showed the same accuracy in terms of mean
423 error as that of SRTM30m. In summary, all the DEMs exhibited negative mean error across all
424 the river basins indicating negative bias or underestimation of the DEMs elevation. In terms of
425 the MAE, SRTM90m outperformed other DEMs in Koshi, Narayani and Karnali While
426 HYDROSHEDS showed better MAE in rest of the river basins (**Figure 14c**). Meanwhile, based
427 on the RMSE, SRTM90 revealed improved performance in Koshi, Kamala, Bagmati, Narayani,
428 West Rapti and Karnali Basins (**Figure 14d**). Similarly, in Kankai and Babai basins,
429 HYDROSHEDS was better while SRTM30m was better in Mahakali in terms of RMSE.

430 The histogram of the elevation errors of the DEMs for Kankai, Kamala, Bagmati, West Rapti
431 and Babai basins are plotted in **Figure 15** (ASTER, AW3D, CARTO and COPERNICUS) and
432 **Figure 16** (HYDROSHEDS, MERIT, SRTM30m and SRTM90m). Similarly, **Figure 17** and
433 **Figure 18** demonstrate the same for Koshi, Narayani, Karnali and Mahakali basins. As in the
434 case of physiographic divisions, the histogram plot of elevation error of each DEMs depicted
435 negative bias across all river basins. The histogram, in general, revealed that the frequencies of
436 negative errors are higher than the positive ones. This meant that the frequencies of the negative
437 errors are positively skewed. However, in the case of Terai, all DEMs except ASTER and
438 CARTO indicated the frequency of positive error to be greater than the negative ones which
439 implied that the frequency of positive errors is negatively skewed.

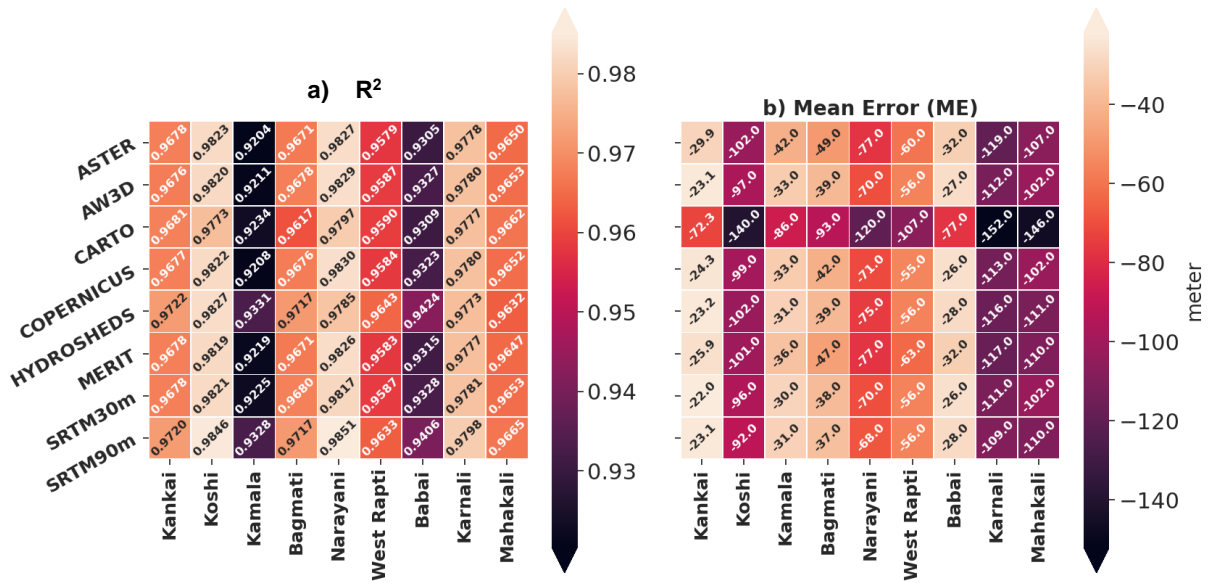


440

441 **Figure 13.** Scatterplot of reference spot elevation versus elevation of different DEMs at

442 corresponding points for the Koshi River Basin.

443

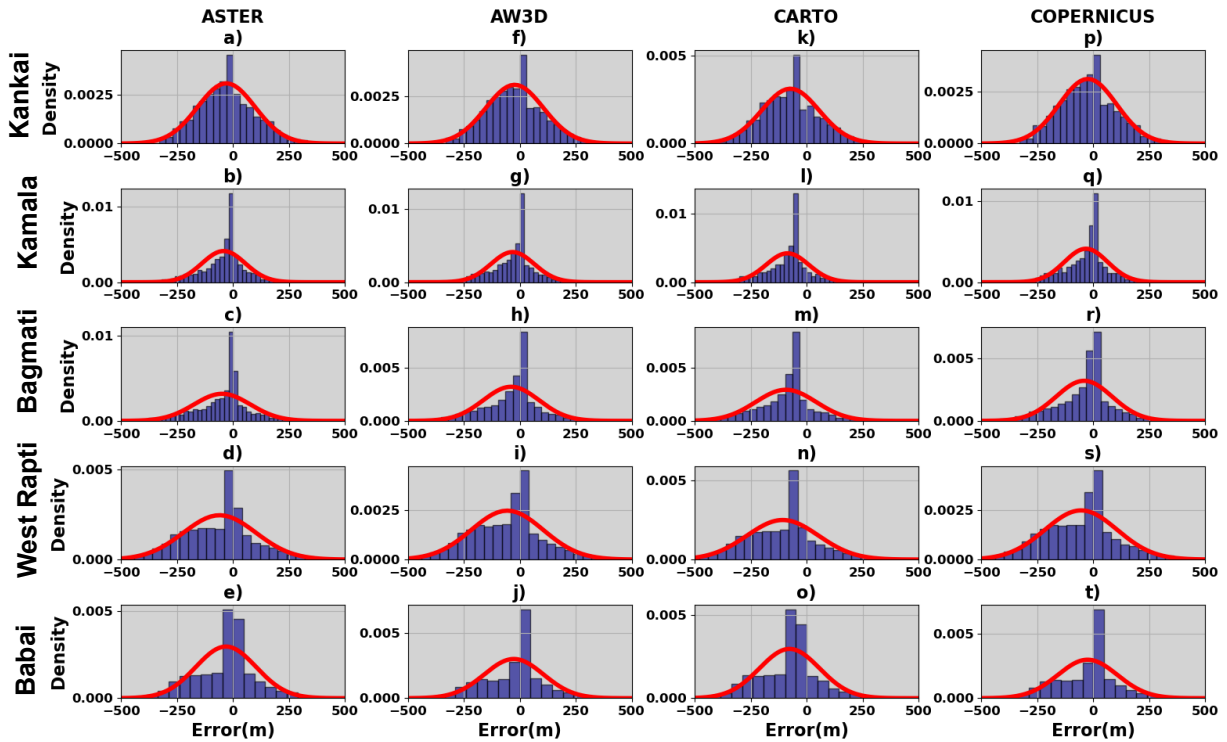


444

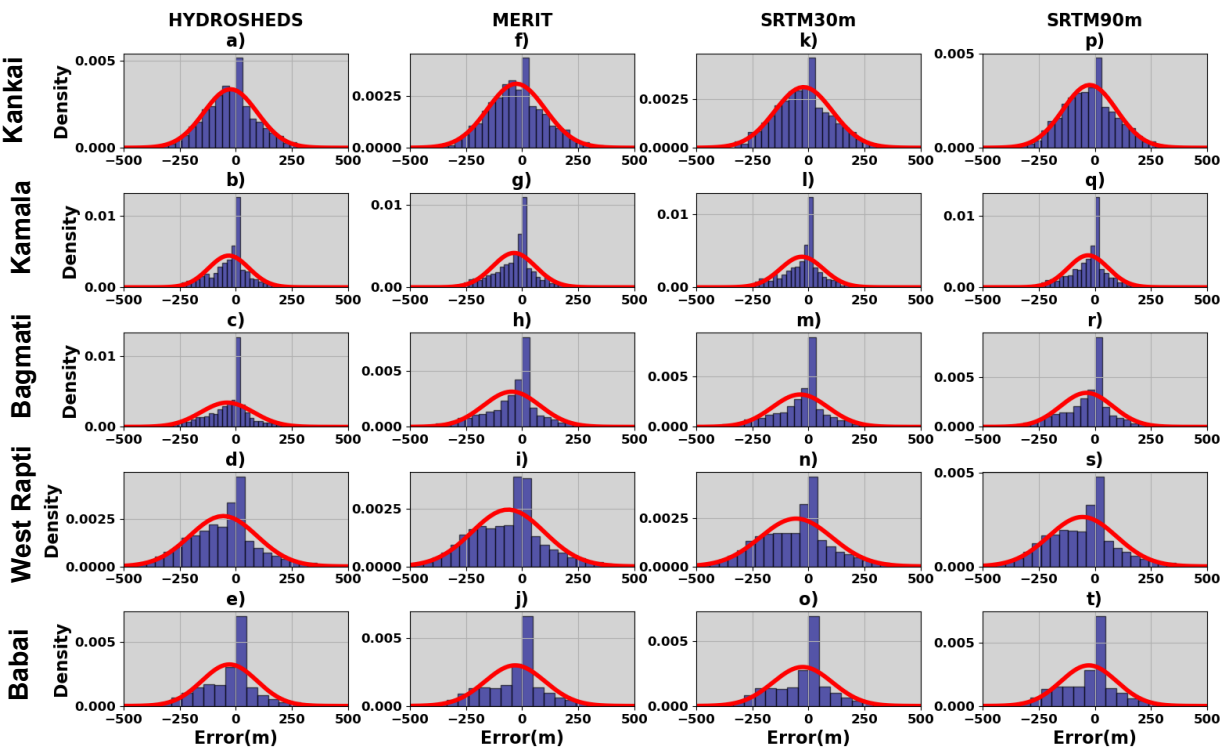


445 **Figure 14.** Comparison of different statistical measurements for each DEMs estimated from
 446 the elevation error across each river basins.

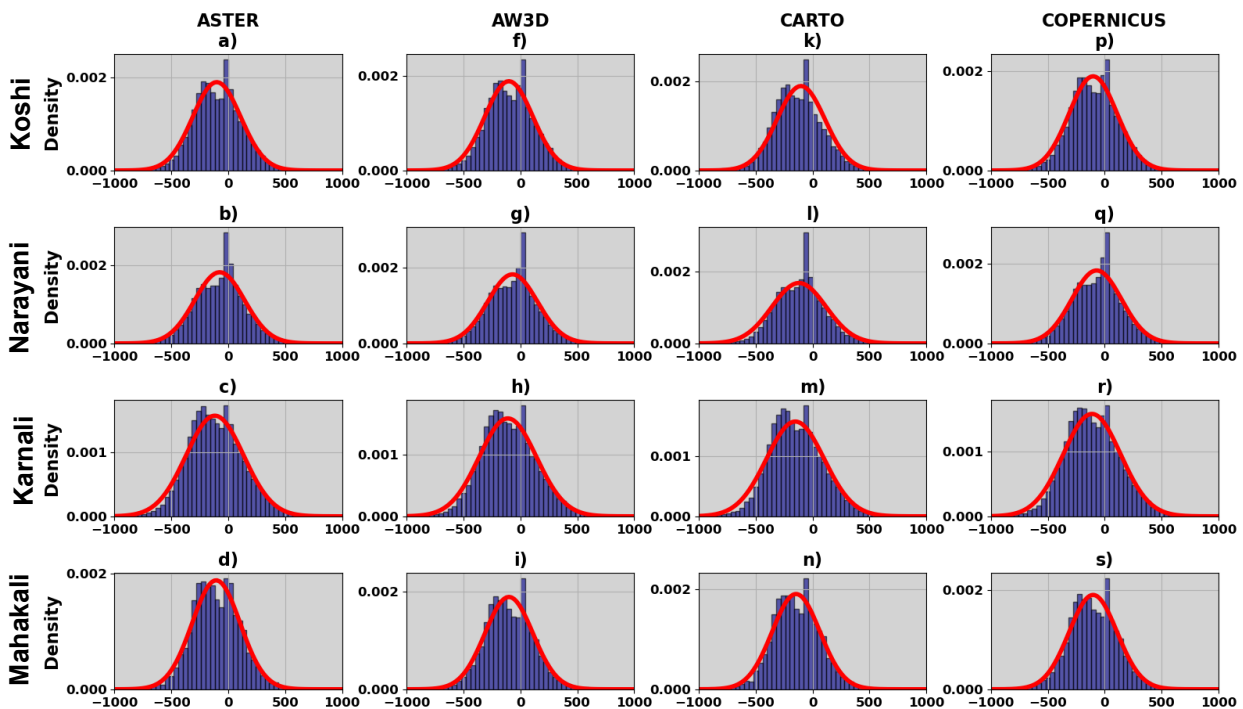
447



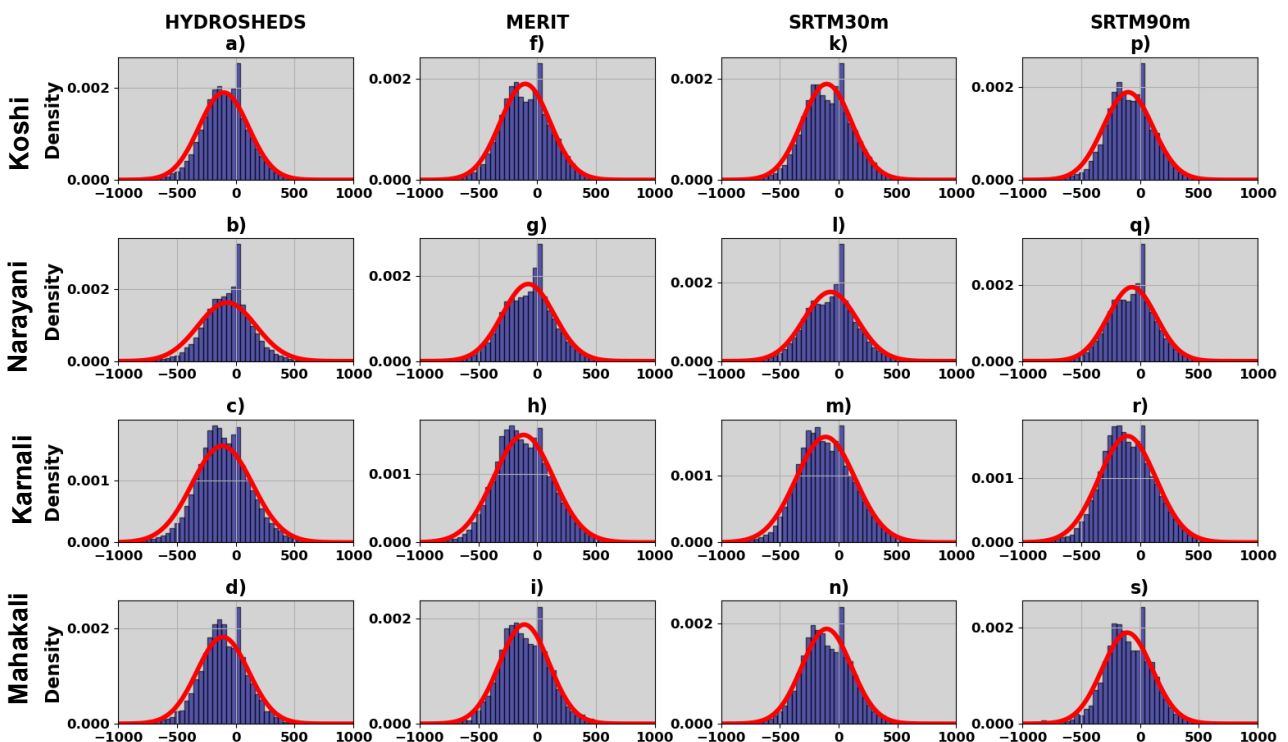
448
 449 **Figure 15.** Histogram of elevation error for ASTER, AW3D, CARTO and COPERNICUS
 450 across five river basins. The red line in the figure represents the fitted curve based on normal
 451 distribution.



452
 453 **Figure 16.** Histogram of elevation error for ASTER, AW3D, CARTO and COPERNICUS
 454 across five river basins. The red line in the figure represents the fitted curve based on normal
 455 distribution.



456
 457 **Figure 17.** Histogram of elevation error for ASTER, AW3D, CARTO and COPERNICUS
 458 across four river basins. The red line in the figure represents the fitted curve based on normal
 459 distribution.
 460



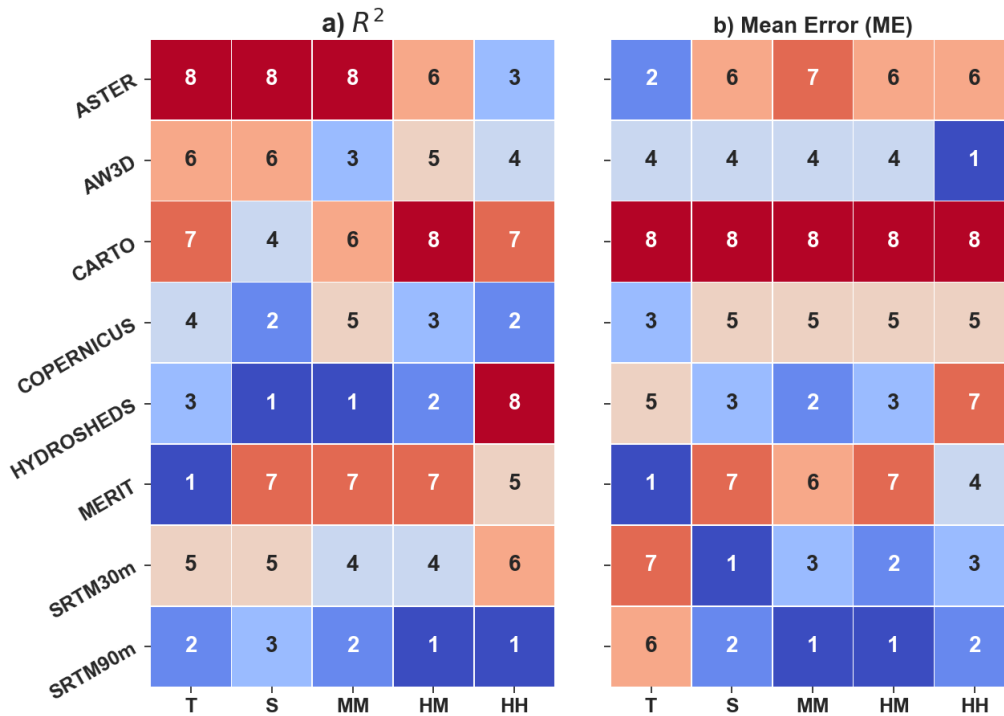
461
 462 **Figure 18.** Histogram of elevation error for ASTER, AW3D, CARTO and COPERNICUS
 463 across four river basins. The red line in the figure represents the fitted curve based on normal
 464 distribution.
 465

466 **4.3 Raking of the DEMs**

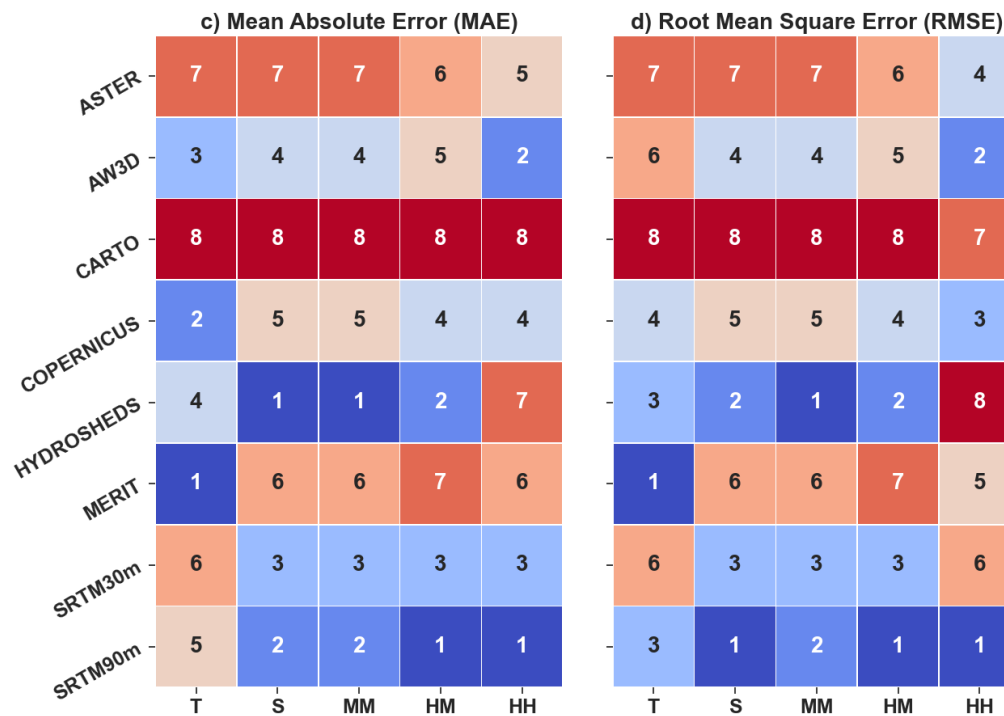
467 *4.3.1 Ranking at the physiographic division*

468 The eight DEMs considered in this study are ranked between 1 to 8 based on their values of

469



470



471



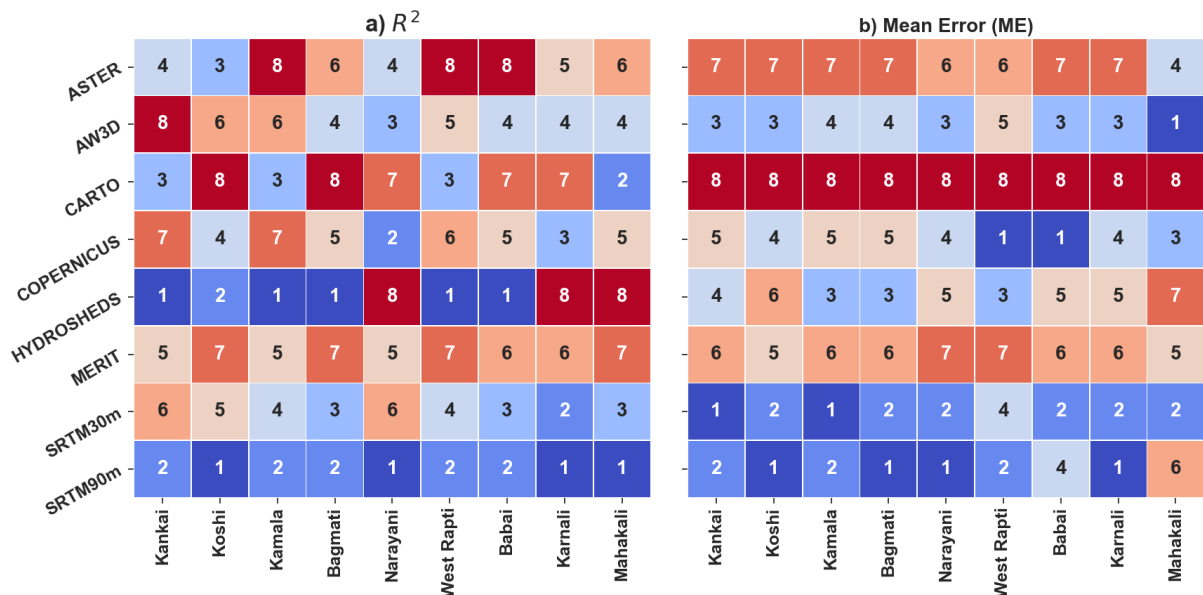
472 **Figure 19.** Ranking of the DEMs across different physiographic divisions based on the
 473 statistical measurements of the elevation error.

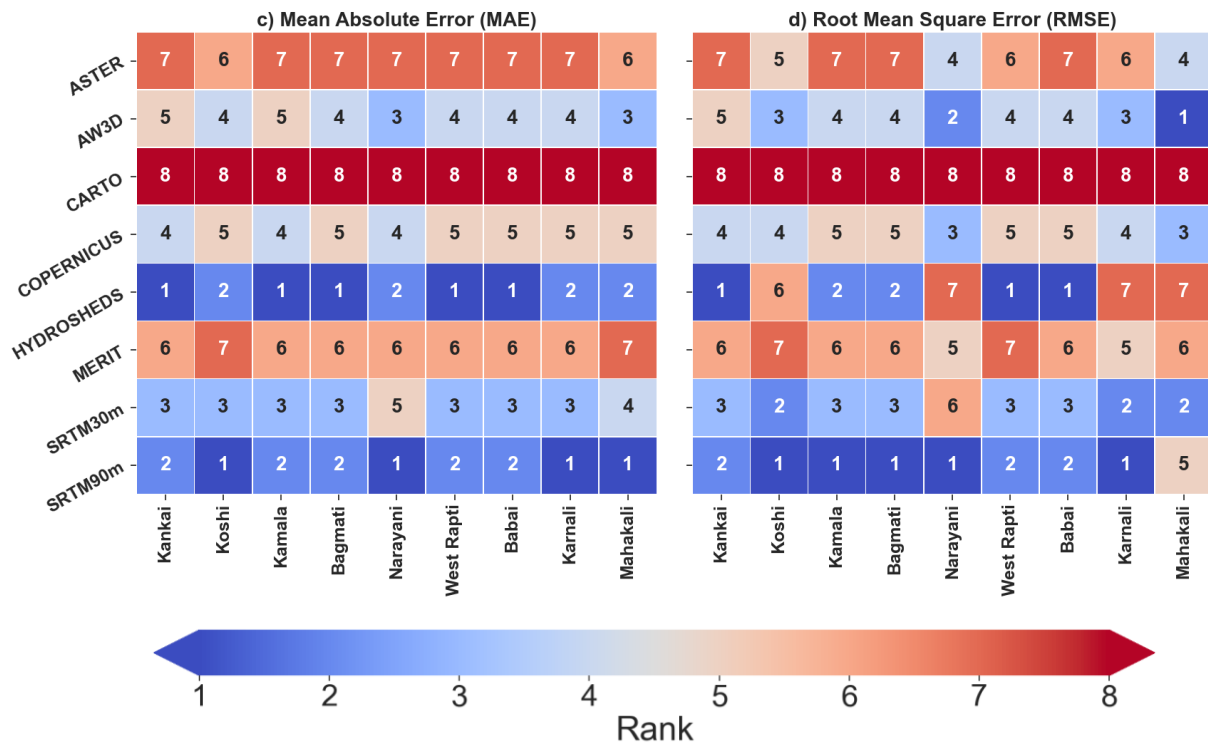
474
 475 error statistics. The four statistical measurements of the error as presented in the previous
 476 section are R^2 , ME, MAE and RMSE. The DEM with higher R^2 value is ranked 1 while the
 477 lowest one is ranked 8. For other three statistics, the DEMs showing the lowest ME, MAE and
 478 RMSE are ranked 1 while those exhibiting the highest values are ranked 8. Accordingly, **Figure**
 479 **19** depicts the rank of each DEMs across different physiographic divisions.

480 Based on all the error statistics, for Terai, MERIT exhibited the best accuracy among all the
 481 DEMs analyzed in this study. In the case of Siwalik, SRTM90m ranked first based on RMSE
 482 while SRTM30m ranked first based on the ME. Similarly, HYDROSHEDS came first in terms
 483 of R^2 and MAE. However, the difference in error statistics values between HYDROSHEDS and
 484 SRTM90m were extremely marginal. HYDROSHEDS also ranked first in three of the four error
 485 statistics in the middle mountains. In high mountain and high Himalayas, SRTM90m proved to
 486 be superior to its other counterpart DEMs in all four statistical measurements.

487
 488 *4.3.2 Ranking at the river basins*

489 As in the case of physiographic divisions, the ranking of different DEMs across different river
 490 basins are prepared based on the values of the measurement of the error statistics (**Figure 20**).





492

493

494 **Figure 20.** Ranking of the DEMs across different river basins based on the statistical
 495 measurements of the elevation error.

496

497 SRTM90m depicted better performance in most of the river basins. In terms of R^2 , it ranked
 498 first in four river basins and second in five basins (**Figure 20a**). Similarly, in four basins,
 499 SRTM90m ranked first based on the ME while in three basins, it ranked second. SRTM90m
 500 also showed first rank in four basins and second rank in five basins in terms of MAE. In all the
 501 basins where SRTM90m came second, HYDROSHEDS ranked number one with a very slim
 502 margin of error. In larger basins Koshi, Narayani and Karnali, SRTM90m by ranking number
 503 one, proved its dominance over other DEMs based on all the error statistics. MERIT DEM
 504 which had shown highest accuracy in Terai region, performed poor at the river basins level.
 505 HYDROSHEDS seems to be preferable in basins like Kankai, Kamala, Bagmati, West Rapti
 506 and Babai along with SRTM90m. While in Mahakali, AW3D showed the number one rank in
 507 terms of RMSE and ME. The issue that needs a few attentions is the performance of
 508 COPERNICUS DEM. COPERNICUS released in 2020 is a relatively new product as compared
 509 to other DEMs and their applicability is yet to be examined in hydrological or geoscience
 510 studies. It ranked number one in couple of basins like West Rapti and Babai in terms of ME. In
 511 terms of RMSE, it ranked third in Narayani and Mahakali. In this regard, it also seems to be a
 512 promising product to be tested. CARTO and ASTER were left far-behind other DEMs in all the
 513 basins.

514 **5. CONCLUSIONS**

515 The application of DEMs is imminent in any studies concerning the topography as it is a
516 fundamental input data for many geoscience studies. High-resolution DEMs are considered to
517 be a vital tool for mapping and modelling different natural hazards and risks that are influenced
518 by topography. The availability and access to space-borne DEMs is ever increasing. The DEMs,
519 however, are not free from errors arising from different sources during the observations. In this
520 context, the choice of the selection of DEMs becomes a tricky issue for its user. Inaccuracy in
521 the input topography will likely influence the results and thus deceive the users and the planners.
522 Against this backdrop, we evaluated the vertical accuracy of eight different DEMs across
523 different physiographic divisions and the river basins of Nepal. Our results revealed that MERIT
524 is superior to other DEMs (RMSE 9m) in the low lying Terai plains of Nepal where the elevation
525 range is lower. In High mountains and High Himalayas having higher elevation range,
526 SRTM90m outperformed all its counterpart under consideration which is in alignment with the
527 findings of the past studies. Meanwhile in Siwalik and middle mountains, SRTM90m and
528 HYDROSHEDS exhibited almost similar RMSE indicating their compatible uses in these
529 regions.

530 The accuracy assessment across different river basins discerned that the accuracy of SRTM90m
531 was above others in larger river basins like Koshi (RMSE 224m), Narayani (RMSE 215m) and
532 Karnali (RMSE 265m) where the range of elevation is greater. In smaller to medium sized
533 basins like Kankai, Kamala, Bagmati, West Rapti and Babai, HYDROSHEDS could be
534 preferable along with SRTM90m. MERIT DEM which had shown highest accuracy in Terai
535 region, performed poor at the river basins level. Meanwhile, CARTO and ASTER were also left
536 far-behind in accuracy than the other DEMs across all the basins.

537

538

539 **Funding:**

540 No funding has been received to conduct this study.

541

542 **Data Availability:**

543 The DEMs data are freely accessible across different web-platform whose source are mentioned
544 in the description. The spot elevation points used in this study is the property of Survey
545 Department of Nepal and cannot be distributed.

546

547 **References**

- 548 Amatulli G, McInerney D, Sethi T, Strobl P, Domisch S. 2020. Geomorpho90m, empirical
549 evaluation and accuracy assessment of global high-resolution geomorphometric layers. *Sci Data*.
550 7(1):1–18.
- 551 Baral TN. 2006. STATUS OF SURVEYING AND MAPPING IN NEPAL. In: Seventeenth
552 United Nations Reg Cartogr Conf Asia Pacific [Internet]. Vol. 6. Bangkok: UNITED NATIONS
553 ECONOMIC AND SOCIAL COUNCIL; p. 5–65.
554 https://unstats.un.org/unsd/geoinfo/RCC/docs/rccap17/crp/17th_UNRCCAP_econf.97_5_CR
555 [P10.pdf](#)
- 556 Bhang KJ, Schwartz FW, Braun A. 2007. Verification of the vertical error in C-band SRTM
557 DEM using ICESat and Landsat-7, Otter Tail County, MN. *IEEE Trans Geosci Remote Sens*.
558 45(1):36–44.
- 559 Boreggio M, Bernard M, Gregoretti C. 2018. Evaluating the differences of gridding techniques
560 for digital elevation models generation and their influence on the modeling of stony debris flows
561 routing: A case study from rovina di cancia basin (North-eastern Italian alps). *Front Earth Sci*.
562 6(November).
- 563 Bricker SH, Yadav SK, M MA, Satyal Y, Dixit A, Bell R. 2014. Groundwater resilience Nepal:
564 preliminary findings from a case study in the Middle Hills [Internet]. [place unknown].
565 http://earthwise.bgs.ac.uk/index.php/OR/14/069_Study_area
- 566 Chhatkuli RR. 2003. Building Spatial Database for NGII in Nepal. *Natl Geogr Mag*
567 [Internet].:1–11.
568 <https://citeseerx.ist.psu.edu/viewdoc/download?doi=10.1.1.210.4440&rep=rep1&type=pdf>
- 569 Chu T, Lindenschmidt K-E. 2017. Comparison and Validation of Digital Elevation Models
570 Derived from InSAR for a Flat Inland Delta in the High Latitudes of Northern Canada. *Can J*
571 *Remote Sens* [Internet]. 43(2):109–123.
572 <https://www.tandfonline.com/doi/full/10.1080/07038992.2017.1286936>
- 573 Coulthard TJ, Neal JC, Bates PD, Ramirez J, de Almeida GAM, Hancock GR. 2013. Integrating
574 the LISFLOOD-FP 2D hydrodynamic model with the CAESAR model: Implications for
575 modelling landscape evolution. *Earth Surf Process Landforms*. 38(15):1897–1906.
- 576 Dhital MR. 2015. *Geology of the Nepal Himalaya* [Internet]. Cham: Springer International
577 Publishing. <http://link.springer.com/10.1007/978-3-319-02496-7>
- 578 DoS N. 2021. Survey Department of Nepal [Internet]. <http://dos.gov.np/>
- 579 DoWRI. 2019. Irrigation Master Plan. Dep Water Resour Irrig.(November).

580 Farr TG, Rosen PA, Caro E, Crippen R, Duren R, Hensley S, Kobrick M, Paller M, Rodriguez
581 E, Roth L, et al. 2007. The Need for Global Topography. *Rev Geophys* [Internet]. 45(2):1–43.
582 http://www2.jpl.nasa.gov/srtm/SRTM_paper.pdf

583 Gesch D, Oimoen M, Danielson J, Meyer D. 2016. Validation of the ASTER global digital
584 elevation model version 3 over the Conterminous United States. *Int Arch Photogramm Remote*
585 *Sens Spat Inf Sci - ISPRS Arch.* 41(July):143–148.

586 Hagen T. 1969. Report on the geological survey of Nepal. Volume 1: Preliminary
587 Reconnaissance. [place unknown].

588 JAXA. 2017. ALOS Global Digital Surface Model (DSM) “ ALOS World 3D-30m ”
589 (AW3D30) Dataset Product Format Description Earth Observation Research Center (EORC),
590 Japan Aerospace Exploration Agency (JAXA). (March):11.

591 JICA. 2020. THE PREPARATORY SURVEY REPORT FOR THE PROJECT FOR THE
592 DEVELOPMENT OF DIGITAL ELEVATION MODEL AND ORTHOPHOTO IN THE
593 FEDERAL DEMOCRATIC REPUBLIC OF NEPAL [Internet]. [place unknown].
594 <https://openjicareport.jica.go.jp/pdf/12356085.pdf>

595 Jing C, Shortridge A, Lin S, Wu J. 2014. Comparison and validation of SRTM and ASTER
596 GDEM for a subtropical landscape in Southeastern China. *Int J Digit Earth.* 7(12):969–992.

597 Lehner B, Verdin K, Jarvis A. 2013. HydroSHEDS Technical Documentation Version 1.2. *EOS*
598 *Trans* [Internet]. 89(10):26. <http://www.hydrosheds.org>

599 Leister-Taylor V. 2020. Copernicus DEM Copernicus Digital Elevation Model Validation
600 Report [Internet]. [place unknown].
601 [https://spacedata.copernicus.eu/documents/20126/0/GEO1988-CopernicusDEM-RP-](https://spacedata.copernicus.eu/documents/20126/0/GEO1988-CopernicusDEM-RP-001_ValidationReport_I3.0.pdf/996b90c4-49b1-0883-5553-4e29a29c4bd5?t=1609340156005)
602 [001_ValidationReport_I3.0.pdf/996b90c4-49b1-0883-5553-4e29a29c4bd5?t=1609340156005](https://spacedata.copernicus.eu/documents/20126/0/GEO1988-CopernicusDEM-RP-001_ValidationReport_I3.0.pdf/996b90c4-49b1-0883-5553-4e29a29c4bd5?t=1609340156005)

603 Ling F, Zhang QW, Wang C. 2005. Comparison of SRTM data with other DEM sources in
604 hydrological researches. *Proceedings, 31st Int Symp Remote Sens Environ ISRSE 2005 Glob*
605 *Monit Sustain Secur.*

606 Mukherjee Sandip, Joshi PK, Mukherjee Samadrita, Ghosh A, Garg RD, Mukhopadhyay A.
607 2012. Evaluation of vertical accuracy of open source Digital Elevation Model (DEM). *Int J*
608 *Appl Earth Obs Geoinf* [Internet]. 21(1):205–217. <http://dx.doi.org/10.1016/j.jag.2012.09.004>

609 Nadi S, Shojaei D, Ghiasi Y. 2020. Accuracy Assessment of DEMs in Different Topographic
610 Complexity Based on an Optimum Number of GCP Formulation and Error Propagation
611 Analysis. *J Surv Eng.* 146(1):04019019.

612 NASA J. 2013. NASA Shuttle Radar Topography Mission Global 1 arc second. 2013,
613 distributed by NASA EOSDIS Land Processes DAAC [Internet]. [accessed 2021 May 23].

614 <https://doi.org/10.5067/MEaSURES/SRTM/SRTMGL1.003>

615 Nikolakopoulos KG. 2020. Accuracy assessment of ALOS AW3D30 DSM and comparison to
616 ALOS PRISM DSM created with classical photogrammetric techniques. *Eur J Remote Sens*
617 [Internet]. 53(sup2):39–52. <https://doi.org/10.1080/22797254.2020.1774424>

618 Pakoksung K, Takagi M. 2016. Digital elevation models on accuracy validation and bias
619 correction in vertical. *Model Earth Syst Environ* [Internet]. 2(1):11.
620 <http://link.springer.com/10.1007/s40808-015-0069-3>

621 Pakoksung K, Takagi M. 2020. Effect of DEM sources on distributed hydrological model to
622 results of runoff and inundation area. *Model Earth Syst Environ* [Internet]. 30(0123456789).
623 <https://doi.org/10.1007/s40808-020-00914-7>

624 Purinton B, Bookhagen B. 2017. Validation of digital elevation models (DEMs) and comparison
625 of geomorphic metrics on the southern Central Andean Plateau. *Earth Surf Dyn*. 5(2):211–237.

626 Rawat KS, Mishra AK, Sehgal VK, Ahmed N, Tripathi VK. 2013. Comparative evaluation of
627 horizontal accuracy of elevations of selected ground control points from ASTER and SRTM
628 DEM with respect to CARTOSAT-1 DEM: a case study of Shahjahanpur district, Uttar Pradesh,
629 India. *Geocarto Int*. 28(5):439–452.

630 Sampson CC, Smith AM, Bates PD, Neal JC, Trigg MA. 2016. Perspectives on open access
631 high resolution digital elevation models to produce global flood hazard layers. *Front Earth Sci*.
632 3(January):1–6.

633 Schumann GJ-P, Bates PD, Hawker L, Neal J, Bates PD, Elkhachy I, Jha R, Purinton B,
634 Bookhagen B, Boreggio M, et al. 2018. The Need for a High-Accuracy, Open-Access Global
635 DEM. *Front Earth Sci* [Internet]. 6(1):1–5. <http://dx.doi.org/10.1016/j.jag.2012.09.004>

636 Sharma CK. 1987. *River Systems of Nepal*. [place unknown].

637 Shrestha BB. 2019. Approach for Analysis of Land-Cover Changes and Their Impact on
638 Flooding Regime. *Quaternary*. 2(3):27.

639 SRTM. 2015. The Shuttle Radar Topography Mission (SRTM) Collection User Guide
640 [Internet]. :1–17. https://lpdaac.usgs.gov/documents/179/SRTM_User_Guide_V3.pdf

641 Takaku J, Tadono T, Tsutsui K, Ichikawa M. 2016. Validation of “Aw3D” Global Dsm
642 Generated From Alos Prism. *ISPRS Ann Photogramm Remote Sens Spat Inf Sci*. III–
643 4(July):25–31.

644 Toutin T. 2008. ASTER DEMs for geomatic and geoscientific applications: A review. *Int J*
645 *Remote Sens*. 29(7):1855–1875.

646 Upreti BN. 2001. The physiography and geology of Nepal and their bearing on the landslide
647 problem. In: *Landslide Hazard Mitig Hindu Kush-Himalayas* [Internet]. [place unknown]:

648 ICIMOD. https://lib.icimod.org/record/21555/files/c_attachment_96_777.pdf
649 Winchell M, Srinivasan R, Di Luzio M, Arnold J. 2013. ArcSWAT Interface For SWAT2012:
650 User's Guide. Texas Agric Exp Stn United States Dep Agric Temple, TX.:464.
651 Yamazaki D, Ikeshima D, Sosa J, Bates PD, Allen GH, Pavelsky TM. 2019. MERIT Hydro: A
652 High-Resolution Global Hydrography Map Based on Latest Topography Dataset. *Water Resour*
653 *Res.* 55(6):5053–5073.
654 Yamazaki D, Ikeshima D, Tawatari R, Yamaguchi T, O'Loughlin F, Neal JC, Sampson CC,
655 Kanae S, Bates PD. 2017. A high-accuracy map of global terrain elevations. *Geophys Res Lett*
656 [Internet]. 44(11):5844–5853. <http://doi.wiley.com/10.1002/2017GL072874>
657 Yan D, Wang K, Qin T, Weng B, Wang H, Bi W, Li X, Li M, Lv Z, Liu F, et al. 2019. A data set
658 of global river networks and corresponding water resources zones divisions. *Sci Data.* 6(1).
659